2020_12_04_ECG_ANALYSIS_REPORT_U

by liuc Central Library

Submission date: 06-Dec-2020 06:19AM (UTC+0300)
Submission ID: 1466036857
File name: 2020_12_04_ECG_ANALYSIS_REPORT_U.pdf (1.16M)
Word count: 15752
Character count: 90793

CHAPTER 1

INTRODUCTION

1.1 Introduction

An ECG (electrocardiogram) records the electrical activity of the heart at rest. It provides information about one's heart rate and rhythm. It shows if there is an enlargement of the heart due to high blood pressure (hypertension) or evidence of a previous heart attack (myocardial infarction). However, it does not show whether one has asymptomatic blockages in the heart arteries or predict the risk of a future heart attack. Since the widespread implementation of electronic health records, Electrocardiogram records, and patient data, including laboratory test results and diagnosis of disease and prescribed drug histories, have accumulated in daily clinical practice. These records are an excellent source of practice-based evidence for evaluating electrophysiological changes on ECGs under many clinical circumstances. Therefore, it is necessary to provide a fast and reliable solution that can analyze the ECG data to provide detailed information of a human to identify and reduce health issues related to the heart. In the medical diagnosis, the electrocardiogram is an essential tool that is extensively used for the diagnosis of cardiac abnormalities. An ECG signal represents the heart's human electrical activity measured by placing several electrodes in some specific locations on the body surface. Generally, for a healthy heart five electrical waves P, Q, R, S, and T are present. The P wave reflects the atrial depolarization, QRS complex shows the ventricular depolarization, and the T wave corresponds to the ventricular repolarization. However, ECG recordings are often affected by various types of noises. These artifacts can be classified in two essential types, high-frequency noises such as Electromyograms signal due to Muscle contraction, Motion artifact due to Electrode Motion, Power Line Interference and channel noise which is additive White Gaussian noise introduced during transmission of ECG signal through channels in Tele-cardiology applications. The second type is the low-frequency noises, including especially the baseline wandering caused by respiration or movement of the instruments during acquisition. The presence of these different kinds of interferences can severely affect the accuracy of diagnosis, which requires a pre-processing step. Therefore, Electrocardiogram signal analysis is one of the most critical steps in any ECG signal processing task.

1.2 Thesis Overview

In this thesis work, we will provide an algorithmic solution to analyze ECG data using the wavelet analysis. There are two of the most widely used transform methods in the ECG signal denoising problem. The first class of methods is the wavelet transform, particularly the discrete Wavelet Transform and the Stationary Wavelet Transform. We will provide a denoising algorithm that will be focused on the removal of additive white Gaussian noise over the ECG data. We are hoping that this study will provide an impact on the analysis of ECG data and help doctors to get a more accurate result on their patients.

1.3 Thesis Objective The main objectives of this thesis has described below.

- To design an algorithm to denoise ECG signal using wavelet transformation.
- To use classification methods to distinguish between the different zones of ECG data.
- To extract QRS peak from ECG signal and analyze information of patients pulse beat per minute from extracted data.

1.4 Report Outline

Six chapters has covered in the course of design and development of this thesis. The chapters and their contents are as follows:

- Chapter 1 is the introductory chapter that gives the overview, motivation and objective of the thesis.
- Chapter 2 is literature review. Previous work related of this thesis has discussed in this chapter.
- Chapter 3 is methodology. In this chapter, the methodology used in this thesis has described elaborately.
- Chapter 4 deals with the system design of the thesis. In this chapter Block diagram, Flow chart and Programming of the thesis has discussed.
- Chapter 5 deals with the system implementation and results, Objective verification and system specification.

- Finally, the summary of this thesis has discussed in detail in chapter 6. The limitation of the thesis, advantage and future development has discussed on this topic.

CHAPTER 2

LITERATURE REVIEW

2.1 Introduction

An electrocardiogram abbreviated as ECG is a test that measures the electrical activity of the heartbeat. With each beat, an electrical impulse travels through the heart. This wave causes the muscle to squeeze and pump blood from the heart. A normal heartbeat on ECG will show the timing of the top and lower chambers. The right and left atria or upper chambers make the first wave called a P wave following a flat line when the electrical impulse goes to the bottom chambers. The right and left bottom chambers or ventricles make the next wave called a QRS complex. The final wave or T wave represents electrical recovery or returns to a resting state for the ventricles. When biomedical signals are recorded, many kinds of noise may appear. Because there exist many different biomedical signals, the electrocardiogram ECG signal was chosen. This signal is well known for a long time, and it is well described in the literature. The ECG signal is almost always disturbed by noise. Examples of noises are 50 Hz power line interference, baseline wander, electromyogram (EMG), motion artefact. Most types of noise are not stationary. It means that the noise power measured by the noise variance features some variability. Muscle noise is the most challenging noise that should be suppressed. White Gaussian noise is usually used to model an EMG signal.

2.2 ECG Denoising Technique

Many authors have demonstrated the solution to solve the noise problems in the ECG signal. They have revised some of these works below.

2.2.1 Automated ECG Noise Detection and Classification System for Unsupervised Healthcare Monitoring

Author Udit Satija et al. has demonstrated that Electrocardiogram (ECG) signals are tainted with various sorts of commotions and ancient rarities, for example, pattern meander and float, for example terminal contact clamor and cathode movement antiques, powerline obstruction, and muscle relics, making it practically difficult to play out a morphological and RR span examination

of such defiled ECG signals.[1]. Most of the existing ECG analysis systems have designed to handle relatively noise-free ECG signals. In such scenarios, existing systems render inaccurate and unreliable measurements, which lead to producing high false alarm rates for the noisy ECG signals. When a signal is decomposed with wavelets, the filters act as an averaging filter or a filter that produces details. Some of the resulting wavelet coefficients correspond to details in the data set. If the details are small, they might be omitted without substantially affecting the main features of the data set. The idea of thresholding is to set to zero all coefficients that are less than a particular threshold. These coefficients are used in an inverse wavelet transformation to reconstruct the data set. Consequently, frequent false alarms are not only the most annoying and disturbing to both the clinicians and the patients but also lead to misdiagnosis of cardiac arrhythmias. The issue of high false arrhythmia event alarm and heart-rate alarm rates highly impacts the usability of real-time ECG monitors because of the two main reasons, i.e., noises and artefacts in the isoelectric line of the ECG signal are falsely detected as normal beats or abnormal beats and severely contaminated ECG beats are misclassified due to the inaccurate measurements of essential ECG feature parameters. Therefore, noisy ECG signals must either be discarded or filtered prior to the extraction of feature parameters. The authors presented a modified complete ensemble empirical mode decomposition (CEEMD) algorithm with new stopping criteria and discussed advantages of the proposed stopping criteria in reducing the computational load significantly as compared to that of the conventional empirical mode decomposition algorithm. Then, they describe the major components of the proposed framework, including the ECG signal and noise separation, the short-term temporal feature extraction, and the decision rules based on noise detection and classification. There are several techniques to decompose an ECG signal into several sub-signals. Empirical mode decomposition (EMD), which is a self-adaptive time-frequency analysis technique, is widely used for decomposing complex, multi-component signal into several fast and slow oscillations called intrinsic mode functions (IMFs). The complete ensemble empirical mode decomposition technique has been proposed to overcome the drawbacks of the basic empirical mode decomposition and ensemble empirical mode decomposition (EEMD), such as mode mixing problem of the basic EMD, where different oscillations exist in the same IMF, or similar oscillations exist in different IMFs. It is producing a varying number of Intrinsic mode functions, and reconstructed signals contain residual noise after decomposition when the signal to noise ratio (SNR) is low. Torres et al. proposed the empirical mode

decomposition algorithm that adds different realizations of Gaussian noise to the residual signal after extracting subsequent intrinsic mode functions. It has been proven that the empirical mode decomposition algorithm provides an exact reconstruction of the original signal and an improved spectral partition of the modes, with a lower computational cost by requiring less than half the sifting iterations that for the Empirical mode decomposition algorithm [2]. By applying the empirical mode decomposition algorithm, a signal is adaptively decomposed into a finite set of intrinsic mode functions (or oscillation modes) and a residue, wherein the decomposition procedure is continued until the obtained residue is no longer feasible to be decomposed (a constant or a monotonic slope, or with only one extremum) or until a predetermined threshold is achieved. The lower-order Intrinsic mode functions capture fast oscillation modes of the high-frequency noises caused by muscle artefacts, power line interferences, and recording instrument noises while higher-order Intrinsic mode functions typically capture slow oscillation modes of baseline wanders.

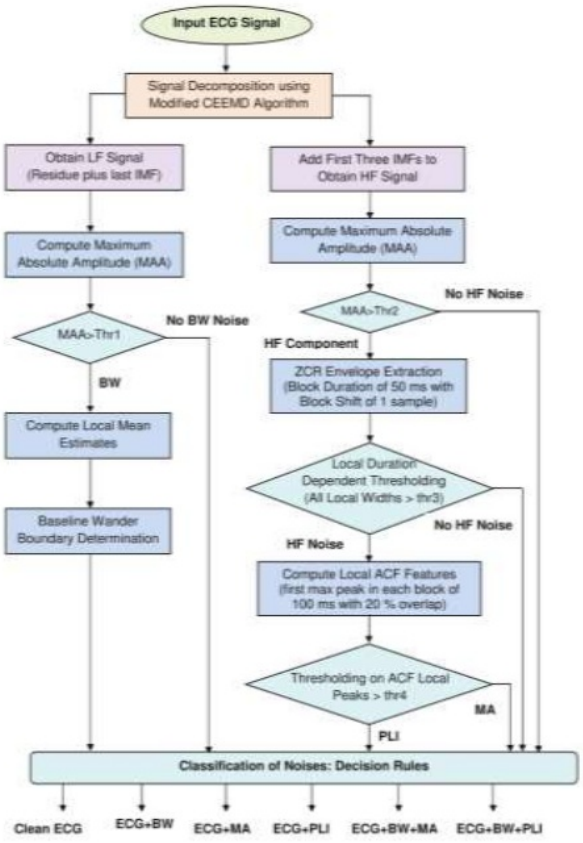

Fig.2.1 Flow Diagram of Proposed System [1]

The final residue represents the trend component of the signal. In this study, they intend to explore the number of zero-crossings and magnitude of the slow oscillation mode of the residue obtained at the IMF extraction process in order to reduce the computational load of the conventional empirical mode decomposition algorithm. In the modified empirical mode decomposition algorithm, the decomposition process is terminated when any following stopping criterion is satisfied. Namely, the magnitude of the current residue is less than the predefined threshold, or the number of zero crossings (NZC) of the current residue is less than the predefined NZC value. The result of the modified empirical mode decomposition algorithm produces a finite set of Intrinsic mode functions and a residue of baseline wander. The predefined threshold values for the stopping criteria are chosen based on the temporal parameters such as maximum absolute amplitude and number of zero crossings of the slow oscillation of the baseline wanders. By considering the baseline wanders with a frequency less than 1 Hz and the magnitude of severe baseline wanders, the NZC of 10 and MAA of 0.1 mV are chosen to discriminate the baseline wanders from the ECG components and the MA and PLI noises.

2.2.2 A Cardiac Electrophysiological Model-Based Approach for Filtering High-Frequency ECG Noise

In this proposed work, author MA Mneimneh et al. approached from the observation of the electric potential of a cardiac cell and specific groups of cells during the cardiac cycle [3]. Substantial research has been done on the internal dynamics of the cardiac cell, they focus this model, for complexity and computational reasons, on characterizing the SA node, the AV node, bundle branches, Purkinje fibres, and left and right ventricles. They have found the cardiac electrical cycle of these groups of cardiac cells is well modelled by the difference of two sigmoids. While other mathematical structures such as polynomials may be used, there is a distinct advantage to the proposed difference of two sigmoids. Only five parameters are needed to model each cell group and these parameters correspond well to physiological characteristics of the heart and also to fiduciary points on the ECG. These parameters are the magnitude, inflexion points, and slopes of the difference of two sigmoids. They correspond, respectively, to the magnitude of electrical activity, the inflexion points of depolarization and repolarization, and the rate of potential change within the cell group. By summing the potential difference of each cell group's electrical activity at

the positive and negative terminals of each lead, the ECG signals are generated. The following sections will present how the ECG wave features are generated. The features are the P wave, the PR segment, the Q wave, the R wave, and the S wave (QRS complex), ST segment, and T wave. The simulated signals are generated from the model developed in. Additionally, white, brown, and pink noise is added to the signal at an SNR level ranging from -25 to 5 dB measured at the ST segment. The process is repeated for 40 trials, and the average mean, the standard deviation of the error, and T wave end variation is measured. Figure 4 represents the noisy signal at -25db white noise.

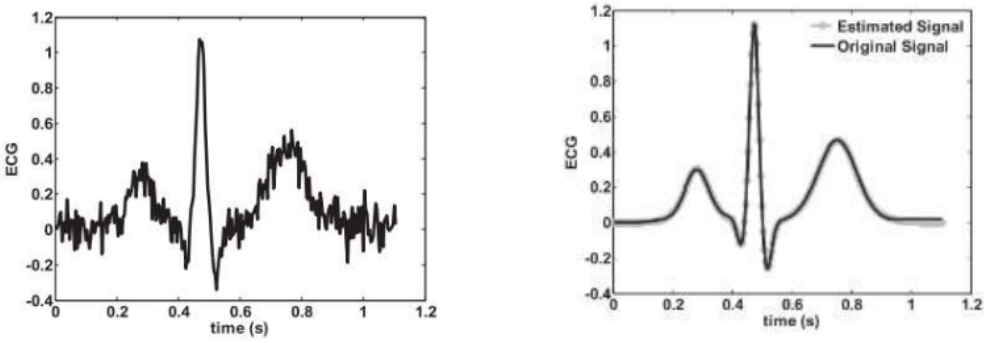

Fig 2.2 The Filtered ECG Signal [3]

Fig 2.2 shows the original signal overlapped by the estimated clean signal. It can be seen than there is an excellent fit between the two. The average mean, standard deviation error between the original and estimated signal, and T wave end variation can be seen that the mean error between the estimated clean signal and the original signal is less than 1%, which is clinically negligible. The standard deviation of 7% is less than 10%, which is also negligible in clinical trials.

2.2.3 ECG Noise Reduction Based on Stationary Wavelet Transform and Zero-Crossings Interval Thresholding

In this proposed method, Mohammed Kalil et al. has extended the interval thresholding method developed by Kopsinis et al. [4] in the SWT domain [5]. The main idea of this approach is that in the case of real environments such as Electromyogram noise, motion artefact and gaussian noise. These kinds of noises will generate more oscillations with a small amplitude, which will cause more zero-crossings in the SWT details coefficients, in contrast to components especially the QRS complex of ECG signal that caused a slow oscillation with a larger amplitude than the noise. Then

they can separate the components of the ECG signal from the noise components at each detail coefficient using the information between zero-crossings. Hence they define a novel thresholding method called SWT Interval Thresholding based on the local extrema (local minima and local maxima between successive zero-crossings in the SWT domain. **Fig 2.3** depicts an SWT decomposition at level 5 using the mother wavelet $'db1'$ of an ECG signal corrupted with a Gaussian white noise with an SNR equal to $5dB$. They notice that from this figure than the most information of the ECG signal is contained in a few coefficients between zero-crossings with a high amplitude. However, the noise is concentrated in a large coefficients between zero-crossings with a small amplitude. As mentioned in the above section, the determination of the optimal value of the threshold that separates the signal information from the noise is one of the unresolved problems in the literature of ECG signal denoising. Normally, in the SWT domain, they have founded that the energy of the sub-bands detail increase where the level of decomposition increases. In contrast, the noise energy decrease in the higher order sub-bands details which contain a useful information of the signal. Based on this observation, the threshold must take a high value for lower order sub-bands (low scale) and a small value for higher order sub bands. In order to achieve this goal, they define a novel adapted threshold called Sign-Uni.

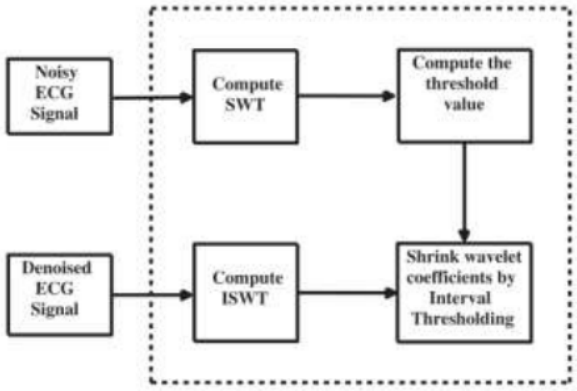

Fig 2.3 A Two Level Decomposition with Stationary Wavelet Transform [4]

2.2.4 ECG Denoising Using Marginalized Particle Extended Kalman Filter with an Automatic Particle Weighting Strategy

The proposed method by Hamed Danandeh Hesar et al. is evaluated using ECG signals taken from the MITBIH Arrhythmia database [6], [7]. It contains 48 recordings sampled at $360Hz$ and

duration of 30 minutes each. The simulations were carried out in MATLAB environment and the comparisons were performed both qualitatively, quantitatively and in the Time-Frequency domain. The EKF/EKS frameworks consider EDM as a nonlinear state-space model and try to recursively estimate the states by linearizing the EDM. This approach has shortcomings in denoising ECG signals in low input SNRs and in non-Gaussian and non-stationary situations. To resolve this problem, in this paper a nonlinear Bayesian filtering framework is presented. Unlike EKF or particle filter, this framework treats EDM as a mixed linear/nonlinear state space model and uses the properties of both particle filter and extended Kalman filter to efficiently approximate the posterior density of ECG and the linear states. Moreover, the proposed scheme has less computational complexity (in comparison to the particle filter approach) and attains better estimations of the linear states in EDM. The experiments showed that in the presence of Gaussian white noise, this proposed framework outperforms the EKF and EKS algorithms in lower input SNRs. They also indicated that it exhibits better results in non-Gaussian non-stationary situations such as the presence of pink noise, brown noise and real muscle artefacts in all input SNRs. In addition, the impact of the proposed filtering method on the distortion of diagnostic features of the ECG was investigated and compared with EKF/EKS methods for four different noise types at four low input SNRs using MSEWPRD metric. The results revealed that this proposed algorithm has the lowest MSEPWRD in all noise types and at low input SNRs and it can conserve the morphology and diagnostic information of the ECG signals much better than EKF/EKS frameworks, especially in non-Gaussian non-stationary situations.

2.2.5 Significance of Modified Empirical Mode Decomposition for ECG Denoising

In the proposed approach, the author Pratik Singh et al. has taken the noisy ECG signal and at first estimated it using the non-local means [8], [9]. The block diagram for the proposed method, which effectively combines the non-local means and modified the empirical mode decomposition method for ECG denoising is shown in **Fig. 2.4**. The non-local means estimation process finds the non-local similarities in the signal using the patches to denoise the ECG signal. Non-local means suffers from the rare patch effect. This leads to the occurrence of under averaged regions in the QRS complex. The signal takeoffs in these regions are not the same as desired. This leads to some morphological dissimilarity between the original and the non-local means denoised signals. On the other hand, the use of a large number of patches in the low amplitude regions for sample estimation leads to over-smoothing. To address this shortcoming, the non local means denoised signal is

further processed via the modified empirical mode decomposition approach in this work. The modified empirical mode decomposition finds the set of Intrinsic mode functions by decomposing the non local means denoised output.

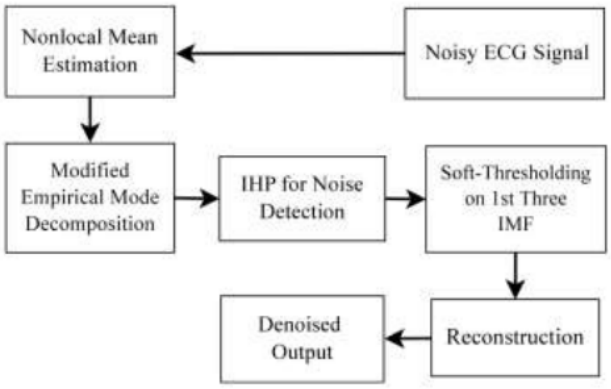

Fig 2.4 Block Diagram Representation of Proposed Method for ECG Denoising [8]

Among those, the first few Intrinsic mode functions contain the more relevant information along with the high frequency noise. To suppress the ill effects of the noise in the IMFs, these are thresholded using IHP and soft-thresholding. Lastly, the reconstruction is done by combining all the Intrinsic mode functions . As a result, the issue of under-averaged QRS complex region due to the rare patch effect are significantly reduced. Moreover, the denoised signal is noted to largely retain the correct morphological characteristics. In the following subsection, they discuss the modified empirical mode decomposition algorithm along with the thresholding techniques employed in the proposed denoising method. The standard empirical mode decomposition process is very well known technique for signal decomposition [10]. At the same time, is also a high latency process due to the large number of iterations involved in finding the individual IMFs. The iterative process in standard empirical mode decomposition involves the calculation of interpolation points (IPs) which are then used for cubic spline-interpolation during the sifting. The way these IPs are calculated can save a lot of processing time and complexity. Exploiting this fact, a modified version of the empirical mode decomposition algorithm has been recently proposed for the tasks related to speech signal processing [11]. The main difference between the standard and the modified empirical mode decomposition process lies in the derivation of the IPs. In the case of the traditional empirical mode decomposition process, the IPs are calculated in each iteration used

for computing the IMFs. But the computation of IPs in the case of the modified empirical mode decomposition process is done from the residue signal. The residue signal is actually a by-product of the iterative process to derive the IMF. As a result, for each IMF, the IPs in the case of modified empirical mode decomposition are computed only once after the completion of the entire iterations. In presented exploration, the Mempirical mode decomposition technique was noted to be almost 15 times faster than the traditional EMD. It is interesting to note that the performances from both the version of the empirical mode decomposition were found to be quite similar in the context of ECG denoising. The decomposed Intrinsic mode functions using the modified empirical mode decomposition technique are shown along with the noisy signal. The higher order Intrinsic mode functions contain both the relevant QRS complex information as well as the noise. Among these, the first three Intrinsic mode functions will mostly contribute for the information relevant to the QRS complex along with some noise. The relevant information from those Intrinsic mode functions can be extracted by a proper thresholding of the initial few IMFs.

2.3 Review on ECG Signal Analysis Techniques

Many authors have approached various methods to process ECG data and produce output from it. We have reviewed some these works below.

2.3.1 Comparative Analysis of ECG Classification Using Neuro-Fuzzy Algorithm and Multimodal Decision Learning Algorithm

In this system, author G. Rajender Naik et al. has proposed a new classification procedure for ECG signals called Multimodal Decision Learning Algorithm and classification by using Adaptive neuro-fuzzy algorithm. The main objective of this work is to show that the proposed method gives the best classification than the existing neuro-fuzzy method [12]. Comparative analysis is carried out for both the methods in terms of parameters like true positive, true negative, False positive, False negative, False rejection ratio, false acceptance ratio, global acceptance ratio, confusion matrix, Kappa coefficient, Sensitivity, Specificity and Accuracy. The main objective of this work is to propose a Decision has adaptive nodes and the remaining second, third and fifth layers has fixed nodes [13]. A new machine learning method for classification of electrocardiogram signal called Multimodal Learning Algorithm and the obtained results, characteristics are to be compared with the existing advanced tool called Adaptive neuro-fuzzy algorithm. **Fig 2.5** shows the basic

flow chart of the process being carried out for feature extraction, selection of the best feature set and classification of ECG signal. For the preprocessing stage a pre-recorded electrocardiogram signal is selected from MIT-BIH database and it is filtered using Gaussian Mean Variant Filtering technique to eliminate noise disturbances like power line interference [14], electrode contact noise and base line drift [15]. For the filtered signal, the features are extracted using Integrated Peak Analyzer [16]. Thirty-three features were extracted and among all the listed features, some are selected as the best based on the contours derived from the proposed method i.e., Intensity Weighted Optimization [12].

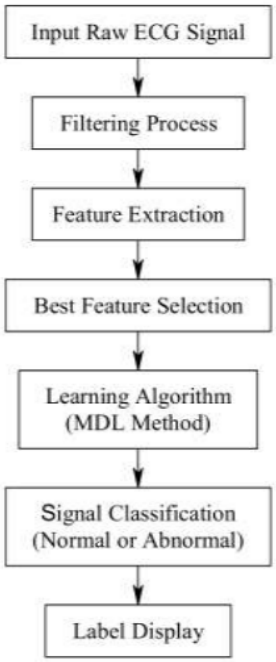

Fig 2.5 Flow Chart of Proposed Methodology [12]

Adaptive neuro-fuzzy algorithm or Adaptive neuro-fuzzy inference system (ANFIS) is one of the hybrid neuro-fuzzy inference system developed by Jyh-Shing Roger Jang. This model is equivalent to a multilayer feed forward neural network but the connections of ANFIS structure just indicates the directions of signal flow between the consecutive nodes without any synaptic weights as in the case of artificial neural networks. The basic first order ANFIS architecture consists of five layers. Out of all the five layers, the first and fourth layers. A method called Multimodal Decision Learning was presented for the accurate classification of any given electrocardiogram signal. The

results are being compared with the most effective adaptive neuro-fuzzy algorithm and the results depict that the proposed model gives the best classification than ANFIS method. Results were presented by comparing with respect to the parameters like true positive, true negative, False positive, False negative, False rejection ratio, false acceptance ratio, global acceptance ratio, confusion matrix, Kappa coefficient.

2.3.2 Analysis of ECG Records Using ECG Chaos Extractor Platform and Weka System

In this proposed system, author Alan Jovic et. al. has collected open sourced data from internet databases, using rdsamp and rdann programs annotations for displaying signal data and data, respectively [17]. They have taken the first minute of signal data and the first half of annotation data. The annotations files contain the exact time and type of the heartbeats, and the signal files contain samples taken at various sampling frequencies, as specified in the table. Both the signal files and the annotations files are input files to the ECE platform. They have not performed any filtering of these records, since they had already been filtered. An automation of the feature extraction process has been performed on the ECE platform. It allows the user to specify a list of input files and the extraction parameters as the input arguments for the platform. The platform then performs the extraction of the specified chaos features and stores them in an output Arff Weka file, ready to be analyzed. The schema of the analysis process is given in **Fig. 2.6**. First, the ECG files are downloaded and prepared. Next, a user starts the ECE platform with specified parameters, including the name of the Weka file to write the results to, the starting point of the analysis, the number of points to be analyzed, the time interval between two consecutive points, the ECG trail number, the m factor for approximate entropy analysis, the list of features to be extracted and finally, the list of ECG files to extract the features from, given by their file path. As the input parameters for the extraction process, they have taken first 500 samples from the ECG signal files and first 500 beats from the annotations files. The 500 signal files samples correspond to a period from one up to this beats of the signal, depending on a record's sampling frequency. They have empirically taken five different intervals between two consecutive points for each record in the databases. For the signal files, they have obtained the extracted data for both trail 1 and trail 2. For the annotations files, since the beat time is equal in both trails, they have specified the m factor 1 and 2 for ApEn evaluation. For the signal files, the platform has been requested to extract SFI, D2 and CTM for each of the trails and for the five intervals. For the annotations files, SFI, D2,CTM and ApEn features have been extracted for each of the m factors and for the five intervals.

Altogether, they have extracted 590 feature vectors from 59 ECG signal files and 590 vectors from 59 ECG annotation files. Total number of vectors per patient. Number of vectors taken from the two trails is the same, as well as the number of vectors with the same m factor: half of total count per class. Since the automatic procedure disregards the real absence or presence of abnormal beats in the extracted time period, they have performed an additional manual extraction for the two disorder patient classes, atrial arrhythmia and supraventricular arrhythmia. They have examined the annotations files for the corresponding disorder beats.

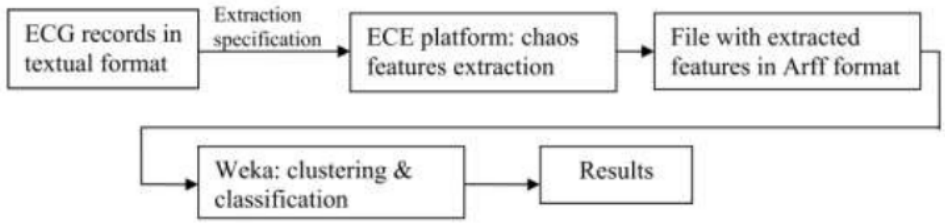

Fig 2.6 ECG Analysis Process Proposed in this System [17]

2.3.3 Identification of Heart Beat Abnormality using Heart Rate and Power Spectral Analysis of ECG

In this system, author Rashima Mahajan et. al. presented the methodology which is implemented in major steps namely ECG signal acquisition, preprocessing, squaring, followed by the determination of R-peaks in corresponding QRS-complexes for heart rate calculation followed by power spectral analysis [18]. A functional block diagram of ECG signal analysis system for efficient and accurate human heart rate measurement and power spectrum estimation to identify heart beat abnormalities is presented in **Fig. 2.7.**

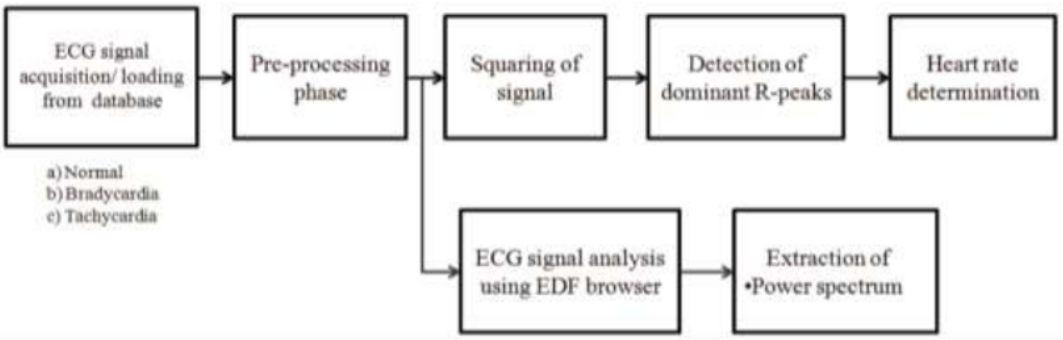

Fig 2.7 Block Diagram Of ECG Signal Analysis System [18]

The filtered signal is squared in order to obtain prominent R-peaks with relatively increased size. The squaring of a signal will emphasize high amplitude R-peaks while simultaneously suppressing low amplitude unwanted and spurious peaks. It increases the discrete values of signal for clearer peak location and identification while carrying out the analysis. Consequently, the R peaks are detected by comparing the adjacent sample values above threshold. Once the R-peaks are detected, heart rate information is estimated by calculating the number of beats per minute. The preprocessing step involves filtering of the signal. The ECG signal record loaded from the database is filtered using high pass FIR filter using the MATLAB functions. A high pass filter with nyquist frequency 1000 Hz and cut-off frequency 1Hz is implemented in order to eliminate low frequency noise (baseline wandering) from input ECG signal. It has been also documented in the literature that heart beat variations are associated with different cardiac states due to age, respiration, varying emotions, mental load, cardiac load, sleep, physical activity, maximum inhalation, hypothyroidism, hypertension, obstructive sleep apnea etc. [19], [20]. An efficient ECG signal analyses method may impart accuracy and reliability to the beat identification system and thus may aid in providing immediate and timely medical assistance. Tachycardia and bradycardia are the most common type of heart beat abnormalities. These are caused by disruption of normal heart impulses which makes flow of blood and oxygen to vital body organs too rapid in tachycardia and too slow in bradycardia. This may lead to heart, brain and other organs damage. In this research paper human heart rate and associated RR-interval information is determined and analyzed for normal, bradycardia and tachycardia ECG rhythms loaded from MIT-BIH arrhythmia database of Physiobank ATM using a concise MATLAB based algorithm with significantly reduced complexity. However, it does not give any information regarding strength of variations and thus distribution of power. Power spectral analysis using the fast Fourier transform is performed to detect and characterize variations in ECG. The conclusions to identify distinct heart beat abnormalities are drawn by correlating the power spectral analysis results with corresponding heart rate information.

2.3.4 Auto Analysis of ECG Signals Using Artificial Neural Network

In this system, the methodology proposed by Abishek Santhosh Raj et. al. is consists of three such as Wavelet Packet Decomposition, Feature Extraction and the classification of signals [21]. This

proposed method was implemented and the automatic analysis of the ECG signal was done with high level of accuracy. The methodology is explained in the following passages. Wavelet Transform is useful in analyzing transient and time-varying signals and hence it is of great use in the analysis of ECG signals. The discrete wavelet transform decomposes the signal into detail signal and approximation signal. The selection of the wavelet function and the number of decomposition levels is very important in the analysis. The selection of these parameters is based on the type of the application and the frequency content. Thus, the wavelet for this proposed method was found to be Daubechies wavelet family, which is similar in shape to ECG signals. Daubechies is normally identified as db. This theory of Wavelet packet decomposition provides a perfect representation of discrete signals. The pre-processing stage which is before the feature extraction is aimed at improving the signal to noise ratio by removing the baseline wander and high frequency noise using filters [22], [23]. Feature extraction is the main part where the necessary features such as entropy, frequency and energy are extracted for analysis. The variations in ECG features like QRS complex morphology and ST-segment deviation and T-wave alternation can be used for the detection of ischemic episodes. Wavelet analysis consists of decomposing a signal or an image into a hierarchical set of approximations and details [24]. Daubechies db4 wavelet is chosen as the mother wavelet since it resembles a heartbeat waveform. The classifier uses a few features to characterize ECG signal as either normal or abnormal. The features extracted are mean, variance, standard deviation, average power, skewness, Median and entropy. The mean of the signal means average of voltages of a signal. This is the statistician's jargon for the average value of a signal, add all of the samples together, and divide by N. Variance is the average of the squared differences from the mean. When a reference to power in a signal is made, it points to the average power. Given the period of a cycle, the power of a periodic signal can be defined. Entropy is a statistical measure of randomness that can be used to characterize the texture of the input signal. The entropy in a signal is inversely proportional to compressibility, the greater the entropy, the smaller the factor by which the data can be compressed. Entropy also refers to disorder deliberately added to data in certain encryption process. Skewness is the measure of the asymmetry of the data around the sample mean. If the skewness is negative, the data are spread out more to the left, of the mean than to the right, if skewness is positive, the data are spread out more to the right. Back propagation is a common method of training artificial neural networks and it is a supervised learning method, and is a generalization of the delta rule [25]. The Back Propagation

method was used to train the neural network and the process is explained below. The set of ECG data, both normal and abnormal signals, were collected from the Physionet database. The features were extracted and trained using the Neural Network Training Tool. Fifty samples each of Normal and abnormal i.e. Myocardial Infarction, Valvular Disease and Pulmonary Embolism ECG data were used in the training with an epoch value of 100000 iterations. After training the Neural Network, testing was performed with 10 other ECG data containing normal and abnormal data of five each and the results were obtained with high accuracy.

2.3.5 Pre Processing the Abdominal ECG signal using combination of FIR filter and Principal Component

PCA is a multivariate investigation technique, which can be utilized for the pre handling of the stomach signal. The dimensionality of the information portrayal can be decreases by utilizing this strategy. In fact, PCA can be considered as a visually impaired source division technique. PCA resembles a rendition of ICA, i.e. the source signals are thought to be Gaussian. Pre preparing utilizing the Principal Component Analysis assists with accelerating the assessment cycle by lessening the quantity of info information viable. In this paper a blend of FIR channels and Principal Component Analysis is acted so as to pre measure the stomach ECG signal. At first the stomach ECG is handled utilizing the FIR channel, and afterward the consequence of this channel is given to PCA stage [26].

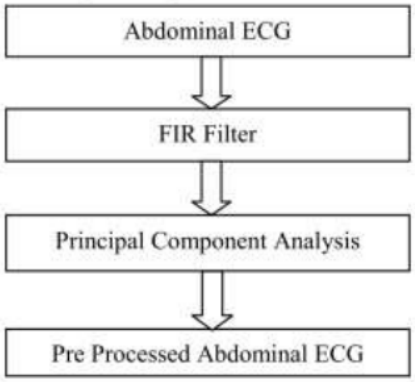

Fig 2.8 Pre Processing the Abdominal ECG signal using combination of FIR filter and PCA [26]

Fig 2.8. shows the square chart of proposed technique. At first the stomach ECG is recorded utilizing direct techniques or aberrant strategies. In direct technique, terminal is gone through

mother's midsection and enter belly to contact the hatchling head. This technique is damaging to both mother and baby. In the roundabout strategy signal is recorded structure mother's mid-region. The recorded ECG is given as the contribution of FIR channel and the consequence of this channel is given to PCA stage. At last the pre prepared yield is acquired which can be utilized for the extraction of Fetal ECG. Butterworth channel is high request channel. It is intended to get a level recurrence reaction in the pass band. It has a maximally level reaction, for example no pass band wave and it has move off of - 20 db for every job. The levelness of the pass band can be improved to the detriment of move off. Butterworth channel is the best trade off among lessening and stage reaction. The Butterworth channel accomplishes its levelness because of moderately wide transient attributes.

CHAPTER 3

METHODOLOGY

3.1 Introduction

For traditional analyzing methods of the ECG, such as visual inspection, the physician notes characteristic visible features within the ECG. An unusual long PR interval, e.g., indicates a conduction defect in the atria, or a prolongation of the QT interval might result in abnormal heart rhythm. Unfortunately, for many medical issues such meaningful features cannot be identified that easily. Additionally, standard features such as the PR interval, the QRS width or the ST level are ambiguous in many cases. As a consequence, sophisticated methods for feature extraction have been used in the literature. These methods try to find new features, which allow drawing conclusions on a patient's medical condition based on the ECG. These features can be extracted from the time domain ECG, the time-frequency domain ECG or the frequency domain. Subsequently these features can then be processed via approaches like visual inspection algorithms.

3.2 Electrocardiogram Characteristics Point Extraction

Visual inspection of an ECG is usually done by evaluating the general shape of the waves and their intermediate segments, followed by measuring the characteristic features. The evaluation of the onset, peak and end of the waves can either be done manually by the physicians or automatically via an algorithm. Manual annotation is time consuming and error-prone due to possible individual interpretations of the experts. Therefore, for a tough morphology of the ECG it often is a matter of opinion where to set the onset and end of waves, even for experienced experts. Although algorithms for automated extraction of ECG characteristic points do not solve this problem, they do have a considerable advantage, namely the reliable detection of relative changes. Detecting a relative prolongation of the QT interval before and after medication. Thus, automated extraction of ECG characteristic points, called ECG delineation or ECG segmentation. Most of the approaches

for ECG delineation are not evaluated on standard databases, which makes their reproducibility and comparability difficult. Approaches like Hidden Markov Model and Neural Network are complex and computationally expensive and often require labeled training sets.

In this thesis we have chosen various properties to make an effort in ECG signal processing. Evaluation on complete standard databases was carried out. Due to the variety of ECG beats in huge databases, the algorithm be able to deal with many different ECG datasets. The algorithm is robust against noise. Hence, ability to detect all characteristic points of an ECG beat is given.

3.3 Electrocardiogram Wave Beat Classification

The heart is basically a muscle divided into four chambers, the left and the right atria as well as the left and the right ventricles. The right atrium collects used blood from the body and forwards it into the right ventricle, which pumps it into the lung. Similarly, the left atrium receives blood from the lung and pumps it into the left ventricle, which consequently supplies the body with oxygen-rich blood. This process can be tracked by ECG, which measures the electrical activity of the heart over time. The ECG signal is an electrical signal, which is acquired at the body surface and reflects the total, time dependent activity of the heart. The transmission of potential changes throughout the heart's conduction system, and the subsequent contraction of the working myocardium can be measured between skin electrodes at the body surface in voltage over the time representing the well established ECG bio signal. Each activation of a heart muscle cell is caused by a distinct change of its initial electrical potential through a membrane bound ion in- and outward flux. Therefore, each activation of a single muscle fiber causes a potential change of the involved cells throughout the myocardium. At a normal heart rate, a cardiac cycle usually lasts about 0.8 s and can be described by five consecutive waves, defined as P, Q, R, S and T wave. Sometimes the T wave is followed by a called U wave. A possible reason for the appearance of a U wave are after-potentials. The distance between two consecutive R waves is called RR interval and can be used to determine the heart rate.

3.3.1 P Wave Classification

If we consider a normal heartbeat, the sinoatrial node fires spontaneously and initiates a heartbeat. Myocardial cells of both atria depolarize causing atrial contraction. As a result, blood is

transported to the ventricles through valves. Atrial depolarization and contraction is visible in the measured ECG, producing the called P wave, while the spontaneous depolarization of the sinoatrial node cannot be tracked. The valves separating the atria from the ventricles prevent the atrial myocardial cells from initiating depolarization of ventricular myocardial cells. Due to this fact, depolarization must be triggered somehow else. For that reason, the depolarization wave travels from the sinoatrial node via the atrial conducting system, the atrioventricular node and the bundle of the ventricular conducting system. The AV node plays a special role in this process by slowing down the depolarization wave and hence delaying the conduction. Due to this, in case of a normal healthy heartbeat, ventricular contraction does not start until atrial contraction is completed and all the blood from the atria is forwarded to the ventricles. This delay is manifested as PR segment in the ECG. Concluding, the P wave describes the excitation propagation in the atria [27]. Usually it is positive and lasts about 110ms. The PR interval, representing the atrioventricular conduction, typically lasts from 120ms to 200ms. Alternations of the P wave's typical shape as well as deviations of time intervals are significant indicators for pathology [28].

3.3.2 QRS Complex Classification

The electrical conducting system of the ventricles is a little bit more complicated than that one of the atria. After the AV node and the bundle of the conducting system splits up into the left and the right bundle branches, and finally ends up in Purkinje fibers, which are responsible for delivering the current to the myocardium. Depolarization of myocardial cells lead to contraction of the cells and consecutive to contraction of the whole chambers. This results in displacement of the blood out of the ventricles. Furthermore, the left branch splits up into three fascicles. Septal depolarization represents the Q wave, which usually appears as small negative deflection in the ECG. Due to the complicated pathway, the QRS complex receives its complex shape [27]. As a result the QRS complex describes the excitation propagation in the ventricles. Its usual width is about 100ms [29].

3.3.3 T Wave Classification

After depolarization of a myocardial cell, it is not possible to stimulate this cell again for a certain amount of time, known as refractory period. The initial ion concentration state between intracellular and extracellular space is restored and the cells can be activated again. The procedure of ventricular repolarization can be detected in the ECG and is manifested as the called T wave.

Extremely small and flat T waves are significant indicators for pathology. Repolarization of the atria cannot be detected since it is superimposed by the QRS complex.

3.4 ECG Wavelet Analysis

Wavelets are described by real or complex value of waveforms, which have a definite beginning and end as well as a mean value of zero. The wavelet transform of a signal is obtained by comparing the input signal with dilated and shifted versions of the unstretched wavelet, the mother wavelet. Due to their limited duration, wavelets are able to deal simultaneously with time and frequency and hence are suited to describe events that start and stop, as it is the case for non-stationary signals. A fundamental goal of signal processing is to extract specific information from a given signal. For that reason signals are often transformed to different domains, expecting that the desired information can be read out easier. One of these transformations is the wavelet transform. The subsequent sections present three major types of the wavelet transform, namely the continuous wavelet transform, the discrete wavelet transform as well as the stationary discrete wavelet transform.

3.4.1 Beat Classification Method

Electrical depolarization and repolarization of the cardiac muscle is described by a pattern of consecutive waves for the healthy heart. Any alternation of this morphological pattern or irregularity of the heart rhythm are indicators for an arrhythmia. Arrhythmia often results from a cardiac disease and is life threatening in the worst case. Thus, automatic recognition and classification of irregularly shaped beats is of great assistance for clinicians, since they can be alerted in case that suspicious beats are detected. In fact, the symptoms of those diseases may not be present all the time, which means that the ECG must be recorded for several hours in order to make a correct diagnosis. One of these irregularly shaped beats indicating a cardiac arrhythmia are called premature ventricular contractions. After optional preprocessing for noise reduction single beats are detected and subsequently used for feature extraction. Potential features are discrete wave tranform coefficients of single beats, subcomponents obtained via independent component analysis r simply time domain features such as the RR interval. In a next step dimensionality of the feature set is reduced with the objective of only keeping the most meaningful features. By selecting the most informative features is a very crucial step for pattern classification, since the

best classifier cannot perform well when poor features are chosen. A classifier, for example based on particle swarm optimization, a support vector machine is trained for recognizing different types of beats. A challenging issue for automated heart beat classification is the inter individual variability of ECGs measured at different patients. These ECGs usually show significant variations in morphology. Hence, performance of the classifier might decrease when a new patient's ECG is analyzed. In order to extract morphological features, discrete wavelet transform using a quadratic spline wavelet of compact support has performed for the single beats. Although the discrete wavelet transform is non-redundant, what is desired for classification tasks that the is better suited in this case due to the discrete wavelet transform lack of time invariance and the resulting sensitivity to the alignment of the signal in time. To reduce dimensionality of morphological features principal component has applied. Additionally to discrete wavelet transform coefficients, RR interval and RR interval ratio has considered.

3.4.2 Beat Changes in ECG

Irregularly shaped heartbeats differ significantly from normal ones in their morphology. However, the ECG might also change in a more subtle way. These changes might not even be visible in the time domain due to the superimposition of high signal deflections or noise. Ventricular late potentials are low amplitude electrical oscillations of limited duration usually occurring after the QRS complex. The reason for these small electrical activities is the delayed conduction of the ventricle muscles. Ventilator late potentials have been used as a predictor for certain types of lethal ventricular arrhythmias. Unfortunately, ventilator late potentials are often masked by noise and hence not visible in the time domain. Since both, the time and the frequency range of these subtle changes is of interest, time frequency analysis seems to be appropriate for detecting and highlighting the wanted information. Among different time frequency analysis methods, the wavelet transformation has shown to be well suited for this task. For the verification of newly developed evaluation methods, it is necessary to start with well-known test signals. If it is of interest whether a known pathophysiology can be quantitatively evaluated by a specific method, a proper ECG test signal containing the desired pathological information is needed. The best case would be to have a synthetic ECG test signal containing exactly the information which is screened for and which is adjustable in any possible way in user defined, arbitrary small steps. Therefore in this work a graphical user interface was developed, making it possible to generate any desired

heartbeat morphology as well as flexible ECG time courses containing user-defined combinations of single heartbeats.

This is realized in an uncomplicated, fast and easy achievable, graphical or parameterized way. Basically it is possible to create any desired heart cycle consisting of maximal six waves and their intermediate segments. In order to obtain maximal variability various waveform parameters, such as magnitude, duration or shape of a single wave, can be altered. Available shapes are a sine half-wave, a bell-shaped curve, a trapezoid as well as the default pattern. Another feature of the generator is to enable or disable any single wave simply by activating or deactivating the according wave. Disabling a wave is realized by linear interpolation between the actual on- and offset point of the wave and subsequent smoothing of the transition points. A very powerful feature of the generator is the possibility to shape all single waves and their intermediate segments simply by dragging and dropping of . For that reason the selected segments are down-sampled by an adjustable factor. A piecewise cubic hermite interpolation is applied between the consecutive Marker points to achieve the user chosen sampling frequency.

3.5 R Wave Detection

The QRS complex is the most striking feature in an ECG and is therefore detected at first. For that reason we search for local positive maxima and negative minima in scale. These maxima and minima are called modulus maxima. Chaining the modulus maxima of the different scales, whereas the modulus maxima lying closest to each other are connected, lead to so called modulus maxima lines. Usually this is performed for the absolute values plotted in a scalogram, however we want to distinguish between positive and negative modulus maxima lines. Hence, modulus maxima lines are determined separately for positive maxima and negative minima. As a first step, the QRS detection algorithm determines modulus maxima lines for modulus maxima with an absolute value greater than a scale dependent threshold. The search for a valid modulus maxima line origins at scale four, since this is the most robust scale regarding high frequency noise and therefore holds the lowest number of modulus maxima. Consequently all modulus maxima of level one to three, which are not within a specific neighborhood of the level 4 modulus maxima, are not considered. In a next step, we want to identify the correct modulus maxima of scale 3 belonging to scale 4 modulus maxima. If there are more than one potential candidates within a neighborhood of

a level four modulus maxima, the one best suited is determined via the following criteria: This prevents the algorithm from taking small local modulus maxima instead of significant modulus maxima just because the small ones are nearer to the L4 modulus maxima. Subsequently the same procedure is carried out for level two and level 1 modulus maxima. By deleting all modulus maxima of scales one to three, which do not have related modulus maxima in the next lower frequent scale, a set of potential modulus maxima lines for R peak detection is obtained. However, there still might be modulus maxima lines not belonging to a QRS complex within this set. These are eliminated through the necessary steps.

3.6 Q and S Wave Detection

After determining the locations of the R peaks, the algorithm continuous by detecting the peak positions of the Q and S waves as well as the onset and end of the QRS complex. Although the typical length of the QRS complex is 110ms, the search window starts 120ms before R and ends 150ms after R in order to allow untypical QRS morphologies. As stated in Q and S waves do have their main frequency content within scale two. Hence, the search for significant modules maxima is performed for this scale. As for the standard QRS complex, the algorithm starts at R, which is bordered by a pair of modules maxima. This pair corresponds to the maximal slopes of the R wave's rising and falling edges. We search for significant modules maxima before R1 and after R2 in order to detect the slopes of the Q and S waves. If there exist more than one significant modules, the one best suited is chosen via a criterion based on the distances to R1 or R2 and the absolute values of the competing modules. Similarly to the determination of the R peak, the according zero crossings at scale one are then used to identify the peaks of the two waves. In order to determine the onset of the QRS complex, the algorithm departs from the earliest significant modules maxima and searches to the left. Afterwards three potential waves for the onset of the QRS complex are identified. The waves lying closest to the R peak that is the most right one is defined to be the onset of the QRS complex. In case that no significant modules are detected, the algorithm simply starts its search for the onset at R1. A similar procedure is performed for finding the end of the QRS complex. Based on the presence or absence of significant modules and on their signs positive or negative, we finally distinguish between the wave regions.

3.7 T Wave Detection

In contrast to the QRS complex, the T wave is a slowly varying signal. Due to this, the search for significant modules is performed at scale four. The search window starts at the end of the QRS complex and its length depends on the current RR interval. Within this search window, a set of significant modules is identified by extracting all modules greater than an interval dependent threshold. The simplest case would be to find one positive and one negative modules leading to the identification of a normal or inverted T wave. The zero crossing between this pair of modules corresponds to the peak of the wave and is identified in scale three due to the better time resolution. But there are some more valid morphological variants of the T wave which are identified by the algorithm. A positive T wave is expressed by a significant positive modules surrounded by two significant negative modules. However, there might be invalid modules within the identified set of modules like two or more consecutive positive modules, modules caused by a discontinuity. These invalid modules are eliminated via the following strategies: modules lines with significant modules in scale one are eliminated since this most probably is some kind of artifact. In case of a T wave, the two surrounding modules must be approximately equal. If this is not the case, one of them is eliminated based on the distance to the center modules and the absolute values of the modules. Finally, the appropriate type of phase is determined and onset as well as end of the T wave are defined via a similar strategy as used for the QRS complex. The algorithm also tries to identify a U wave within a specific search window following the T wave.

3.8 P Wave Detection

The detection and delineation of the P wave is very similar to the process described for the T wave. The main differences are the use of smaller thresholds and that only four different regions are distinguished such as normal, inverted, positive and negative biphasic. The identification starts at the end of the T wave or U wave, in case that this wave exists and ends at the beginning of the QRS complex. The PR interval is an important clinical parameter for the assessment of conduction disturbances. Minimal changes of the PR interval over time might provide important information regarding the patient's state of health for the physician. Hence, it makes sense to detect minimal relative changes of the PR interval. ST segment elevation can be an important indicator for anterior

or myocardial infarction as well as for ischemic cardiac diseases. Therefore minimal relative changes of the ST level also provide important information for the physician. The dataset simulates the patient's ECG at a specific event and the second simulates the ECG after a specific event.

CHAPTER 4

SYSTEM DESIGN

4.1 Introduction

This chapter includes system design and simulation of this project. Flowchart of the system as discussed below.

4.2 Software Requirements

- MATLAB R-2020a: MATLAB combines a desktop environment tuned for iterative analysis and design processes with a programming language that expresses matrix and array mathematics directly. It includes the Live Editor for creating scripts that combine code, output, and formatted text in an executable notebook. MATLAB toolboxes are professionally developed, rigorously tested, and fully documented.
- Signal Processing Toolbox: Signal Processing Toolbox provides functions and apps to analyze, preprocess, and extract features from uniformly and no uniformly sampled signals. The toolbox includes tools for filter design and analysis, resampling, smoothing, detrending, and power spectrum estimation. The toolbox also provides functionality for extracting features like change points and envelopes, finding peaks and signal patterns, quantifying signal similarities, and performing measurements such as SNR and distortion. One can also perform modal and order analysis of vibration signals. With the Signal Analyzer app one can preprocess and analyze multiple signals simultaneously in time, frequency, and time-frequency domains without writing code; explore long signals; and extract regions of interest. With the Filter Designer app one can design and analyze digital filters by choosing from a variety of algorithms and responses. Both apps generate MATLAB code.

4.3 Data Collection

- Physionet Database: PhysioNet includes collections of cardiopulmonary, neural, and other biomedical signals from healthy subjects and patients with a variety of conditions with major public health implications, including sudden cardiac death, congestive heart failure, epilepsy, gait disorders, sleep apnea, and aging.

4.4 Programming

The programming of this whole has system has described in brief below.

- load(filename) loads data from filename. If filename is a MAT-file, then load(filename) loads variables in the MAT-File into the MATLAB workspace. If filename is an ASCII file, then load(filename) creates a double-precision array containing data from the file.
- extractfield: Field values from structure array. Extracted field values, returned as a 1-by-n numeric vector or cell array. n is the total number of elements in the field name of structure a cell array if any field values in the field name contain a character vector or if the field values are not uniform in type; otherwise a is the same type as the field values. The shape of the input field is not preserved in a.
- findpeaks: The function findpeaks(data) returns a vector with the local maxima (peaks) of the input signal vector, data. A local peak is a data sample that is either larger than its two neighboring samples or is equal to Inf. Non-Inf signal endpoints are excluded. If a peak is flat, the function returns only the point with the lowest index.
- mean: The function mean returns the mean of the elements of A along the first array dimension whose size does not equal 1. If A is a vector, then mean(A) returns the mean of the elements. If A is a matrix, then mean(A) returns a row vector containing the mean of each column.
- lowpass: This MATLAB function filters the input signal x using a lowpass filter with normalized passband frequency in units of π rad/sample.
- fprintf: This MATLAB function applies the format spec to all elements of arrays A1 to An in column order, and writes the data to a text file.

4.5 Flow Chart

The overall flowchart of the system has descried in the **Fig 4.1**. We will load the ECG file initially for processing. Every ECG files are sampled at different rate.

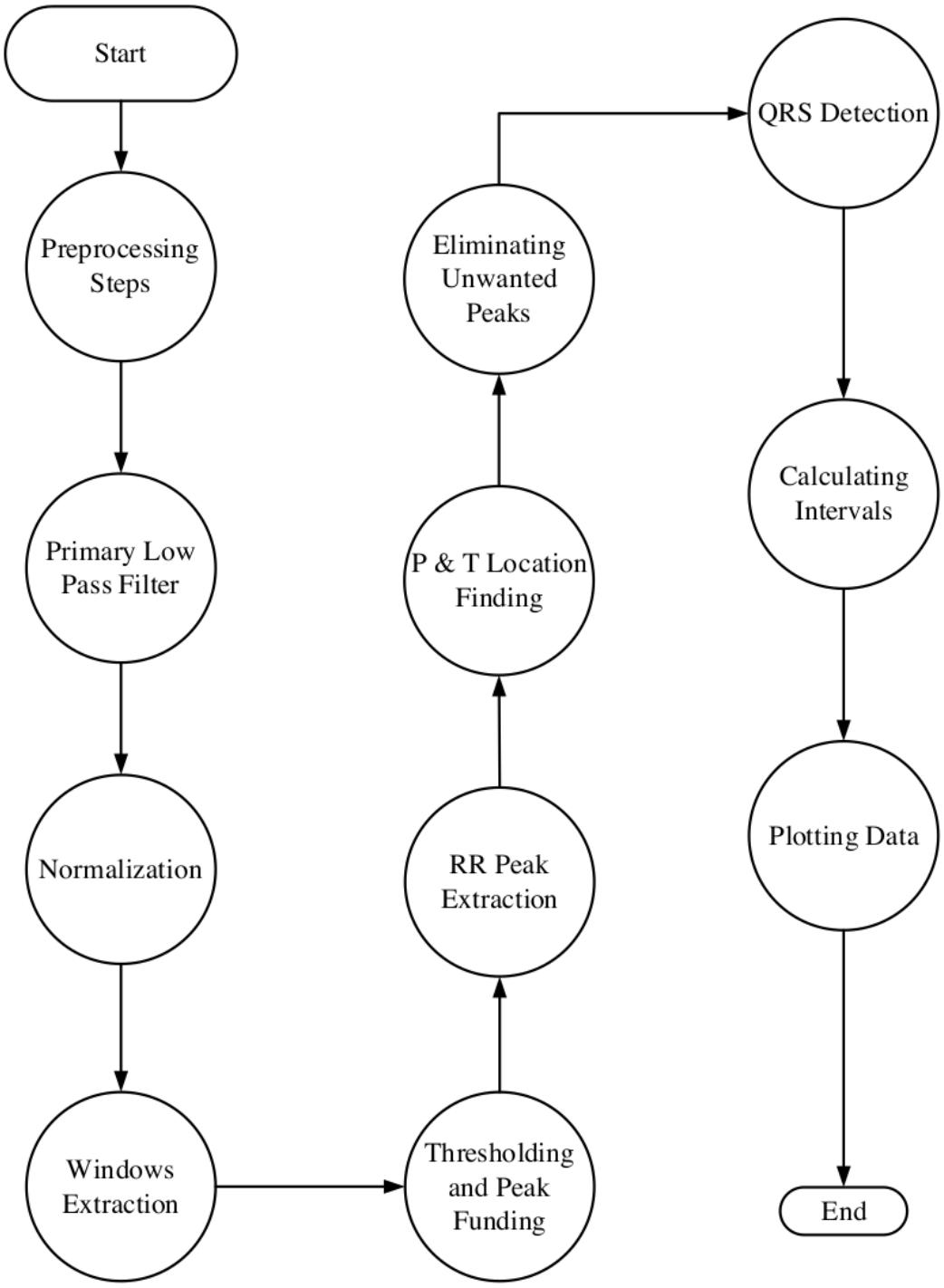

Fig 4.1 Overall Flowchart of the System

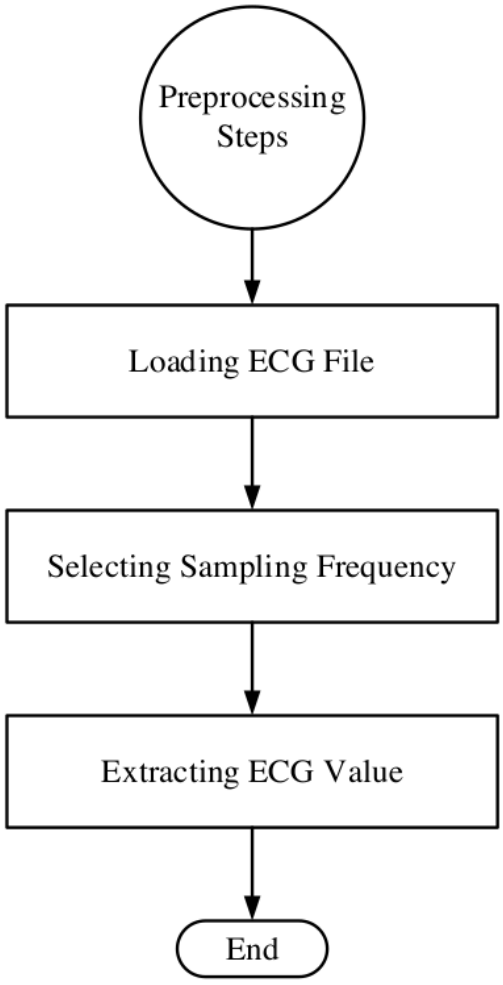

Fig 4.2 Preprocessing Steps Sub process

On our case, the MIT database has sampled at a rate of 360Hz. We have used the ECG ID database as well, which has samples as 500Hz. Then as shown in **Fig 4.2** we will extract the ECG values from the dataset by using MATLAB commands to a variable. After preprocessing step, we have passed through our signal into a primary low pass filter to filter out the noise and smoothing our input signal. As shown in **Fig 4.3** we have selected the input ECG signal and then we have selected the passband frequency for the filter to apply it on the input. The output will be then processed for further information extraction of the system.

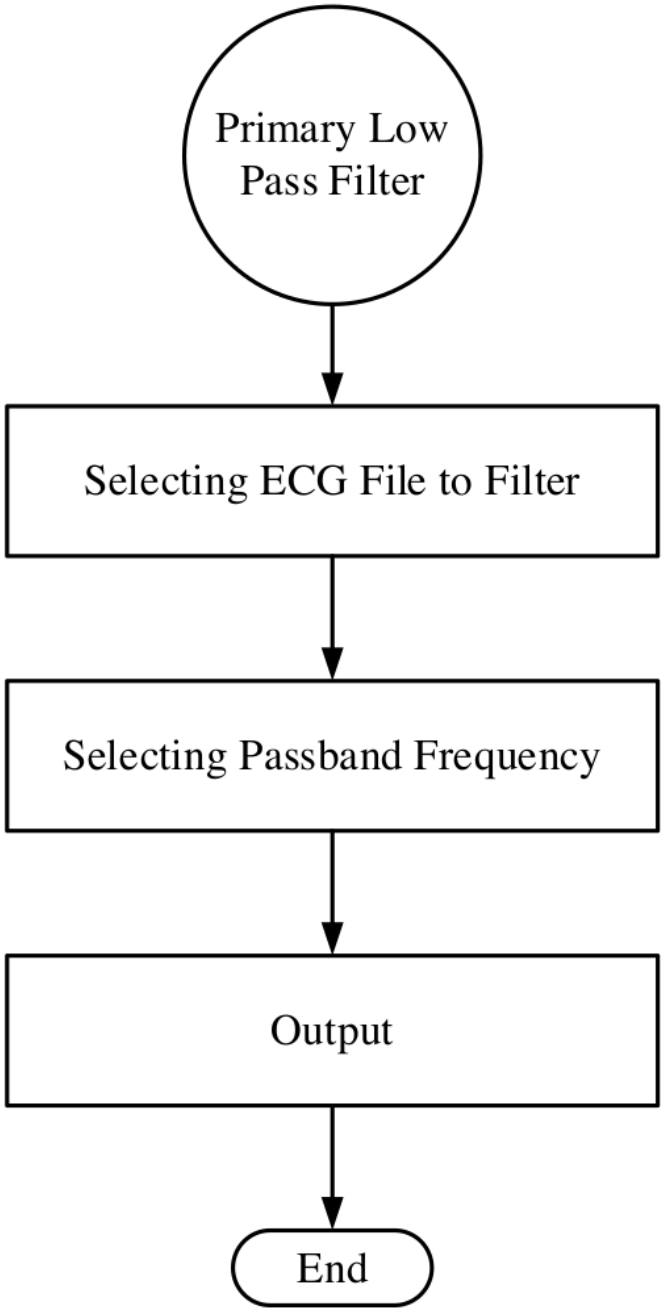

Fig 4.3 Primary Low Pass Filter Sub process

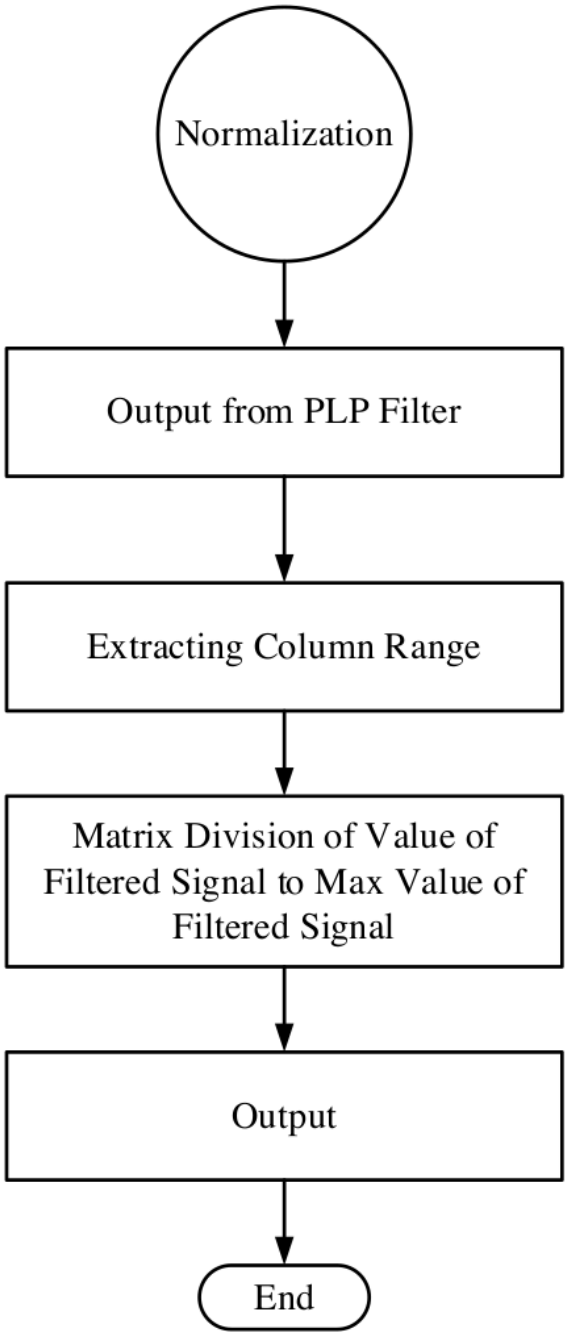

Fig 4.4 Normalization Sub process

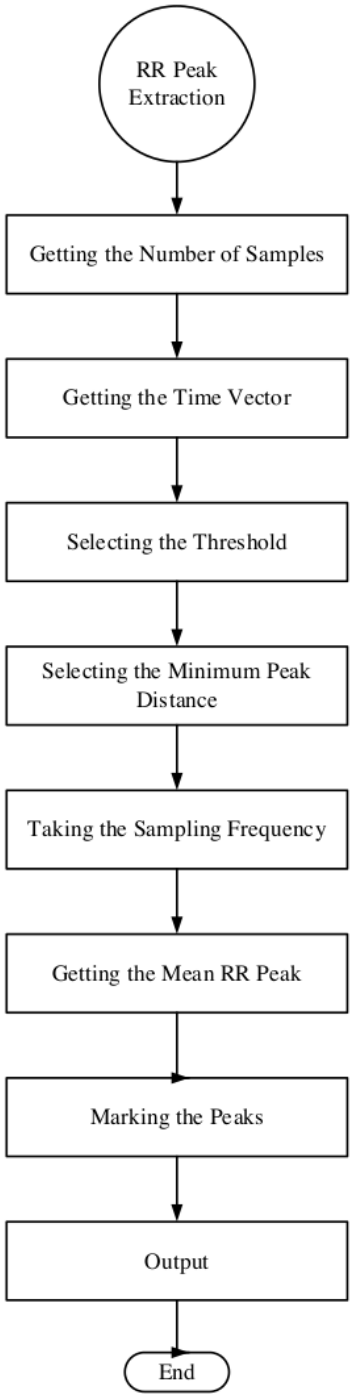

Fig 4.5 RR Peak Extraction Sub process

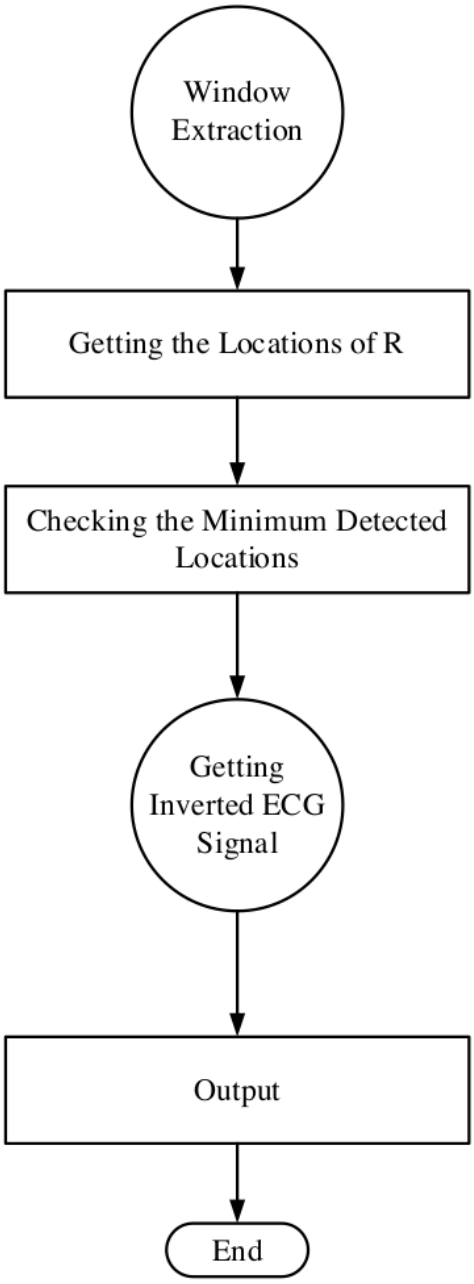

Fig 4.6 Window Extraction Sub process

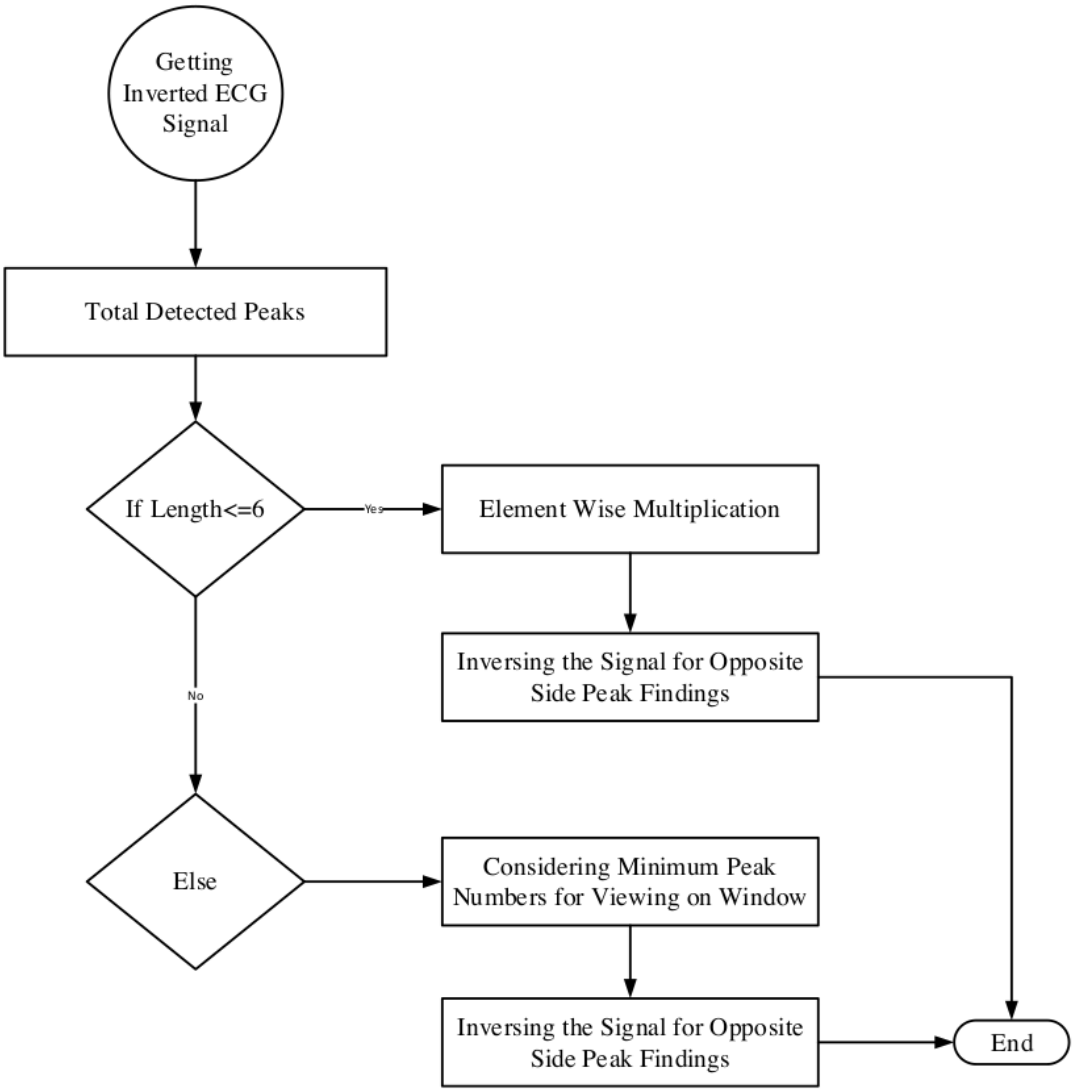

Fig 4.7 Getting Inverted ECG Signal Sub process

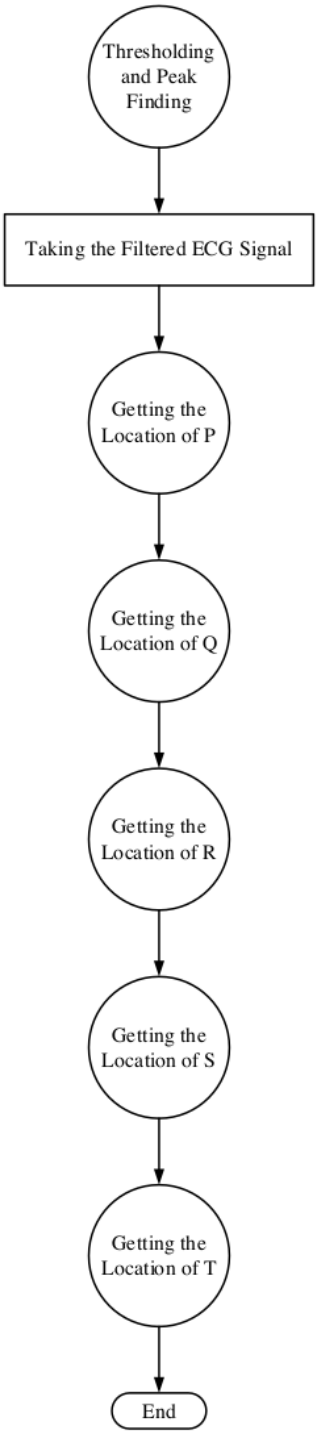

Fig 4.8 Thresholding and Peak Finding Sub process

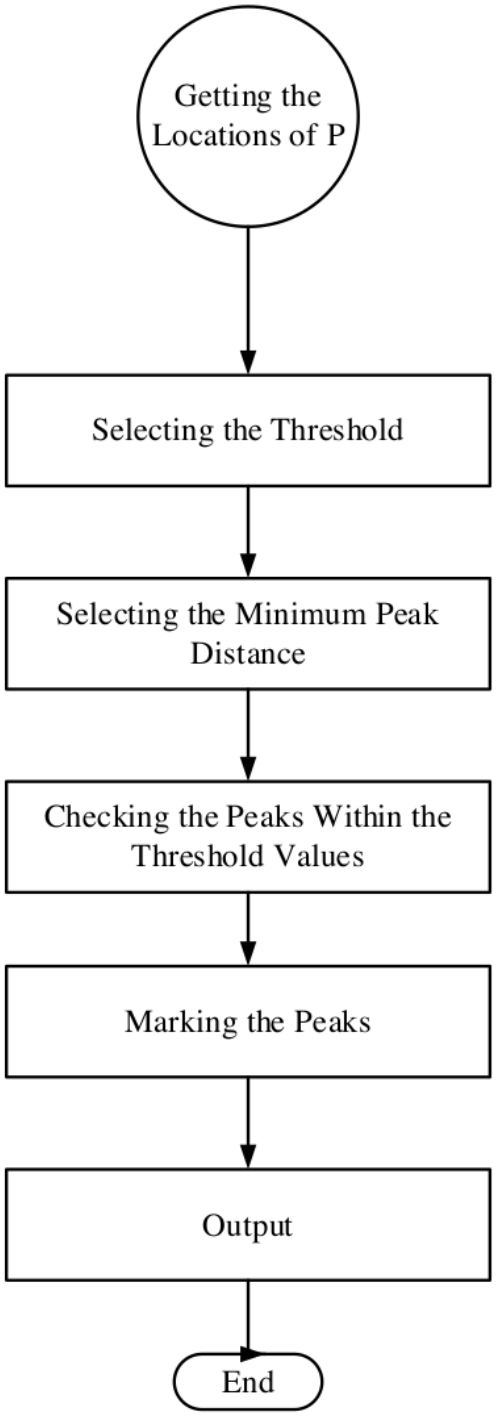

Fig 4.9 Getting the Location of P Sub process

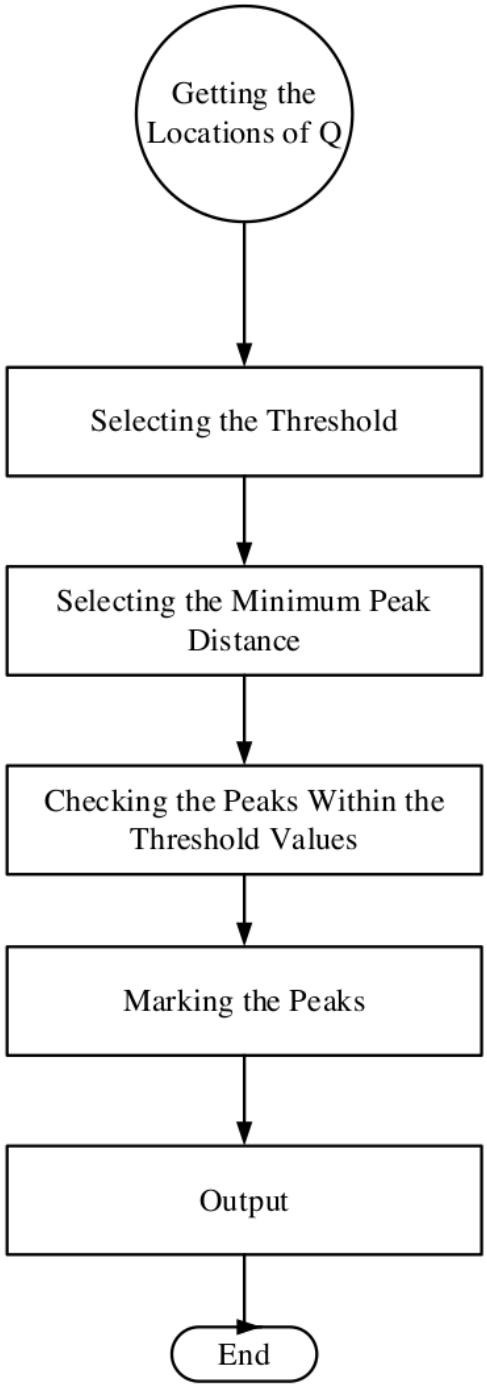

Fig 4.10 Getting the Location of Q Sub process

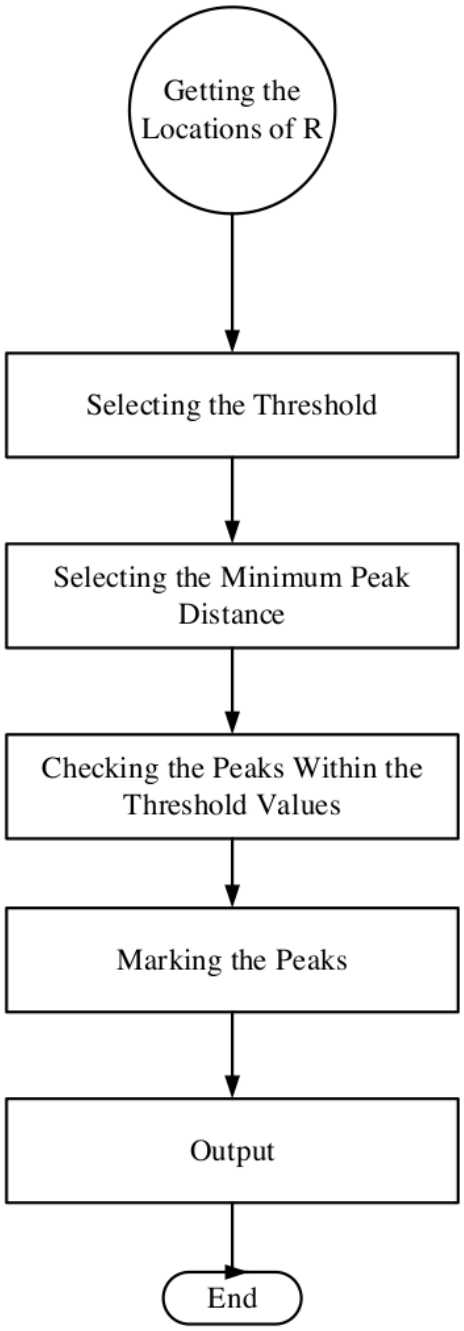

Fig 4.11 Getting the Location of R Sub process

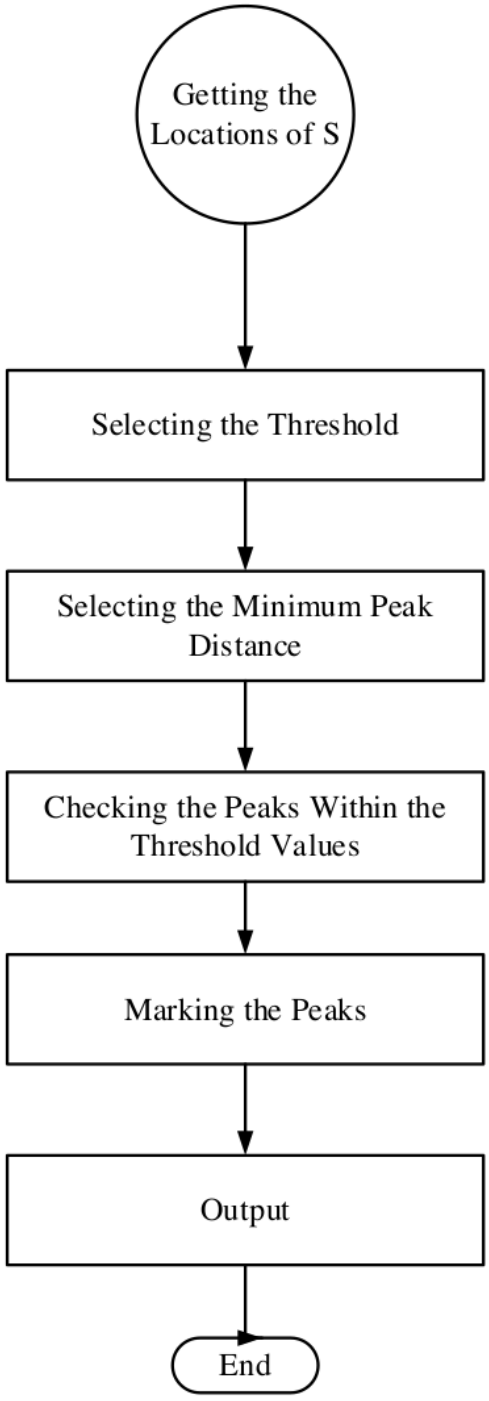

Fig 4.12 Getting the Location of S Sub process

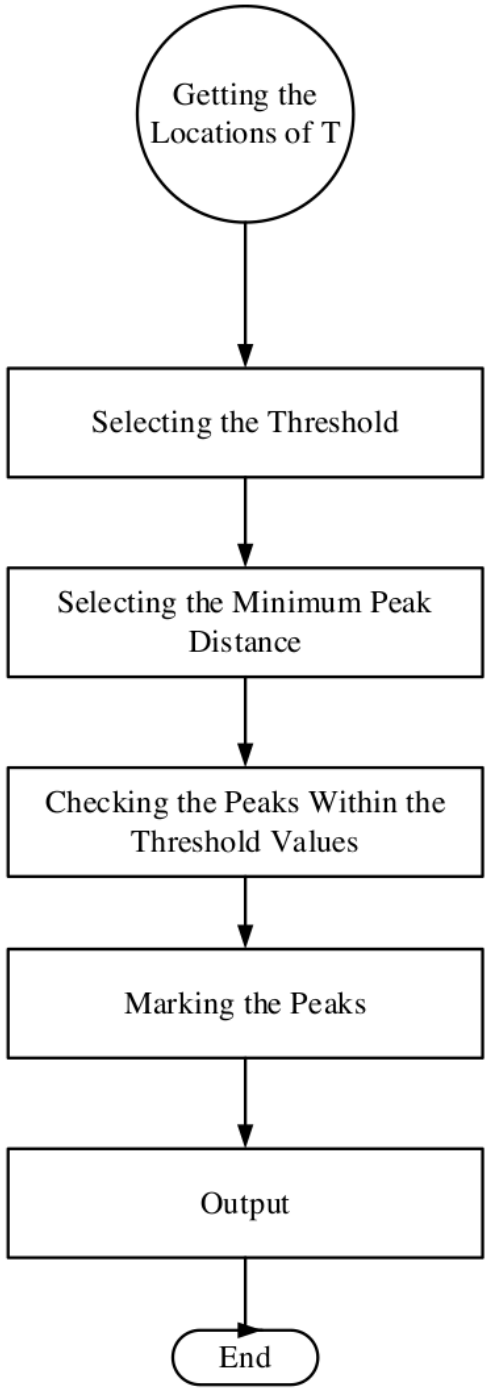

Fig 4.13 Getting the Location of T Sub process

We will extract a certain column range to process the signal further. Then to perform normalization, we will do matrix division the value of each signal by the maximum value that will obtain by the filtered signal within the column range as shown in the **Fig 4.4**.

We will extract a specific number of peaks from the input ECG files to simplify the process of individual region extraction. This will help us to zoom in the signal to find the locations more preciously. For the purpose of window extraction, we will detect the RR peaks initially as these peaks are clearly visible than other peaks of the ECG signal spectrum. We will input the numbers of desired samples as well as the time vector of the signal. To measure the RR peaks number, we will use a suitable threshold. After the threshold selection, it is necessary to select the minimum considerable peak distance to eliminate the unexpected noise occurrence and hence that can leads to the false RR peak detection. Anything within the range of the minimum threshold and minimum distance will be eliminated. By calculating the signals with the respect of sampling frequencies, we will calculate the mean of the RR peak as shown in **Fig 4.5**.

After getting the RR peak extraction we will determine the locations of each R peaks and hence that will help us to check the minimum detected locations by using conditional logic operator. After that we will, invert the ECG signal to double check the correctness of ECG signal. As discussed in **Fig 4.7,** we will check the length of the detected signal. In that case, if the length in less than or equals to six detected peaks, the system will perform a element wise scalar multiplication. Otherwise, we will consider the minimum peaks to display in the viewing window. After these operations, we will invert the opposite peak findings and fed the output to the system as shown in **Fig 4.6**.

After window extraction, we need to identify the individual peaks from the ECG signals as shown in **Fig 4.8**. We will take the filtered ECG signal to identify locations of P, Q, R, S, and T from the input. The peak detection procedure is almost same for the each peaks, however the peak range, distance and threholding value changes with respect to peak location.

To detect the location of each peaks, we need to chose the appropriate value for threshold and the minimum peak distance between them. The algorithm checks the corresponding peaks within the range of values that have mentioned in this range. After peak detection the detected peaks will be marked on the plotted graph for individual graphs. The peak detection procedures are demonstrated in **Fig 4.9** to **Fig 4.13**.

CHAPTER 5

SYSTEM IMPLEMENTATION AND RESULT

5.1 Introduction

In this chapter, the complete implementation and objective justification have discussed with proper demonstration.

5.2 Objective Justification

In this chapter we have discussed the output from our analysis of our thesis. The results are categorized below.

Table 1 ECG Analysis of Patient 1

No.	Figure Properties	Corresponding Figure
1	Input ECG File: 100m (2).mat Database: MIT Database Sampling Frequency: 360 Hz	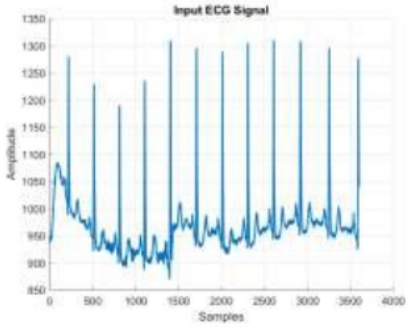
2	Extracted ECG Signal after filtering	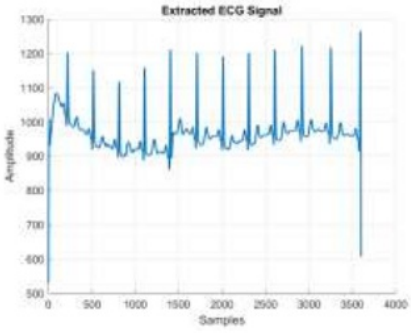

3	Extracting few peaks for better identification	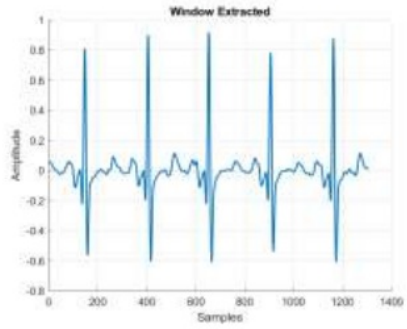
4	Inverting the signal for S peak extraction	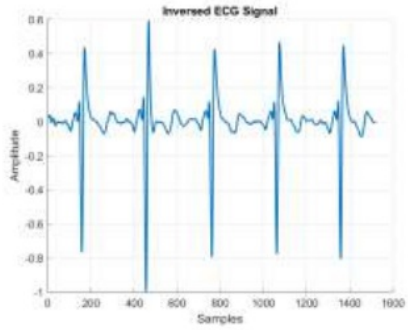
5	Detected P regions on the signal	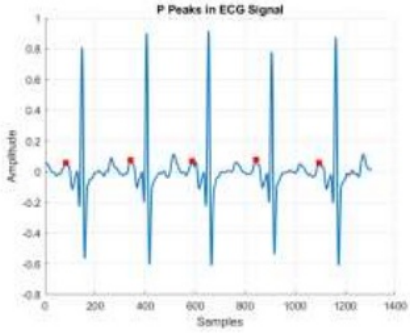
6	Detected R peaks in ECG	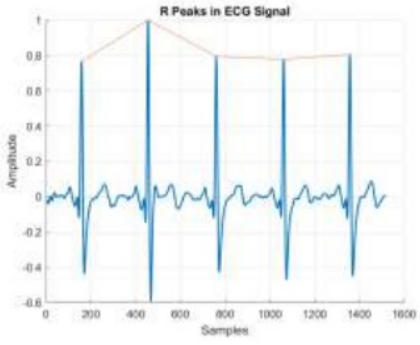

7	Detected S Peaks in ECG	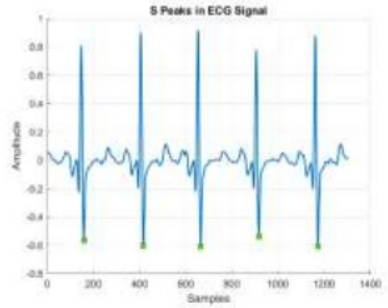
8	Detected T peaks in ECG	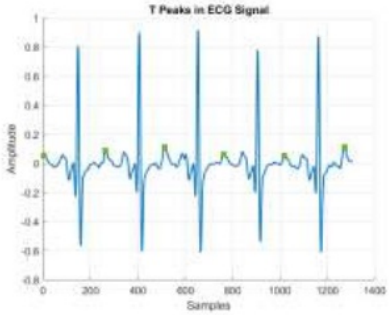
9	QRS Regions for generating BPM	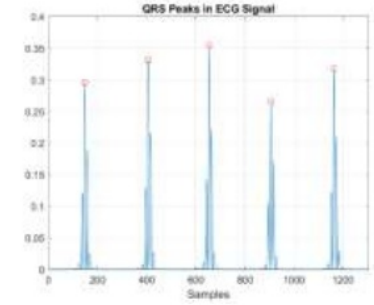

Table 2 ECG Analysis of Patient 2

No.	Figure Properties	Corresponding Figure
1	Input ECG File: 101m (0).mat Database: MIT Database Sampling Frequency: 360 Hz	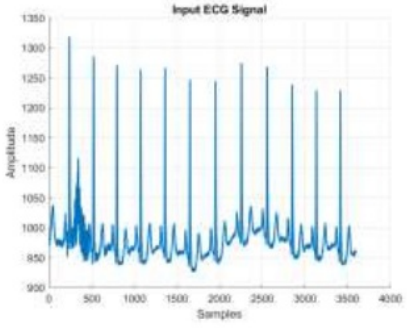

2	Extracted ECG Signal after filtering	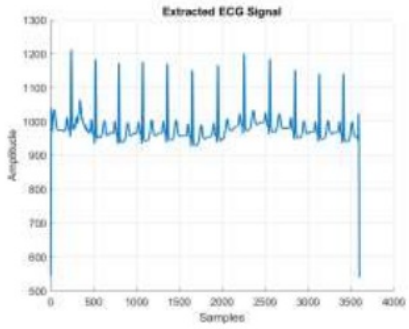
3	Extracting few peaks for better identification	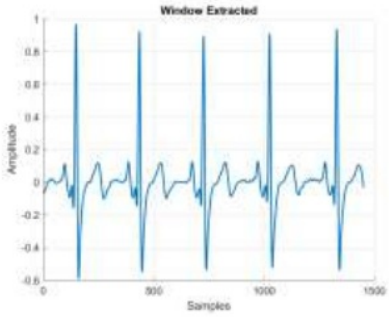
4	Inverting the signal for S peak extraction	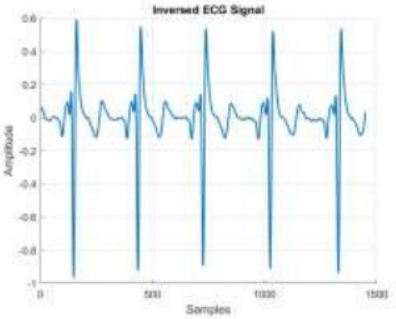
5	Detected P regions on the signal	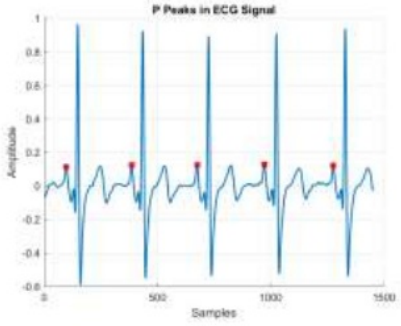

6	Detected R peaks in ECG	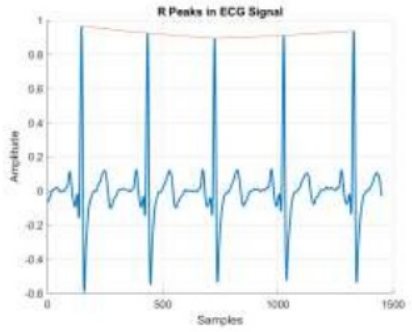
7	Detected S Peaks in ECG	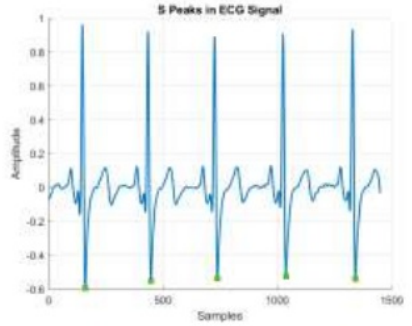
8	Detected T peaks in ECG	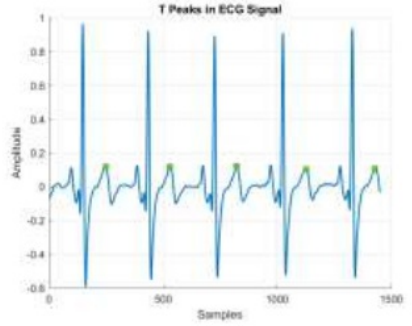
9	QRS Regions for generating BPM	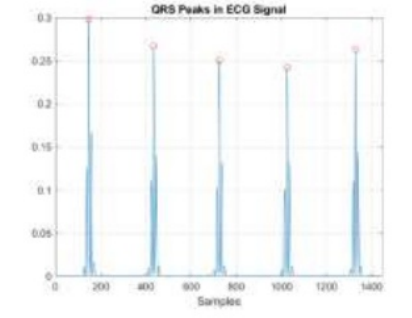

Table 3 ECG Analysis of Patient 3

No.	Figure Properties	Corresponding Figure
1	Input ECG File: 103m (1).mat Database: MIT Database Sampling Frequency: 360 Hz	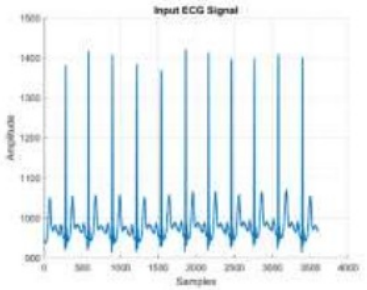
2	Extracted ECG Signal after filtering	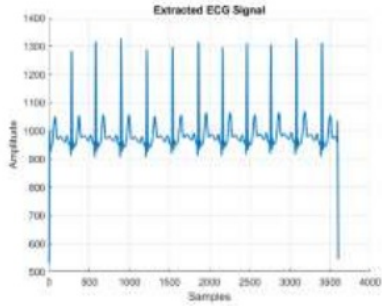
3	Extracting few peaks for better identification	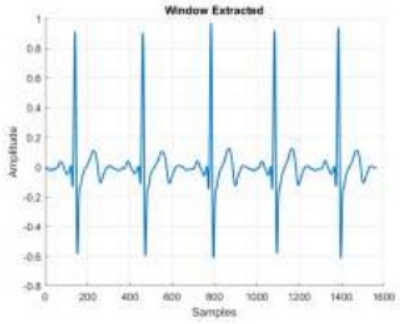
4	Inverting the signal for S peak extraction	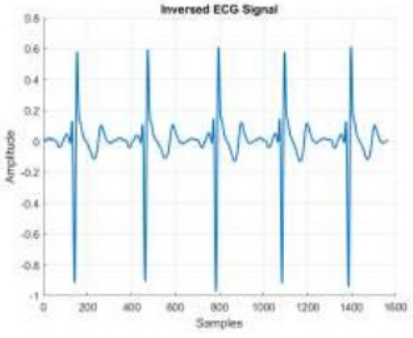

5	Detected P regions on the signal	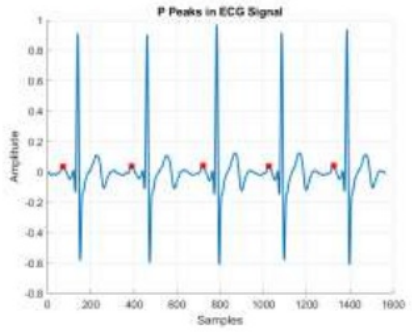
6	Detected R peaks in ECG	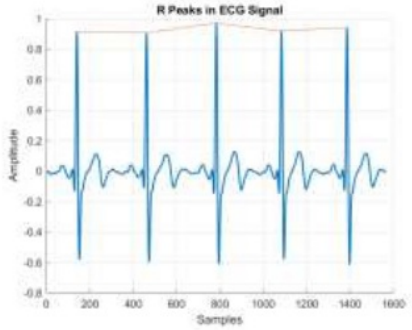
7	Detected S Peaks in ECG	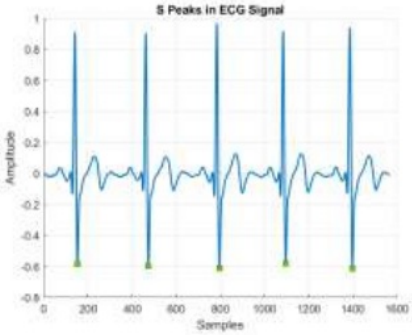
8	Detected T peaks in ECG	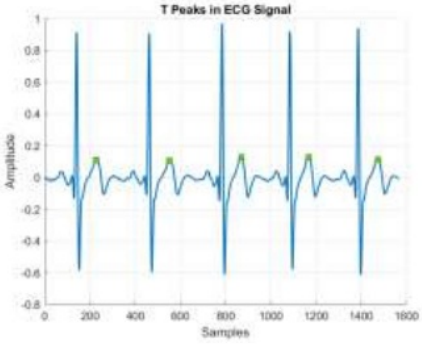

9	QRS Regions for generating BPM	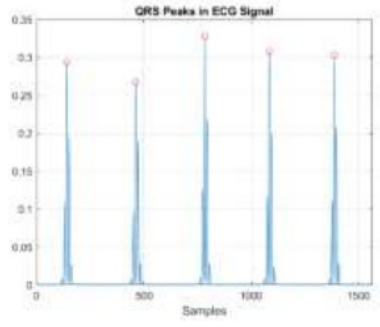

Table 4 ECG Analysis of Patient 4

No.	Figure Properties	Corresponding Figure
1	Input ECG File: 103m (3).mat Database: MIT Database Sampling Frequency: 360 Hz	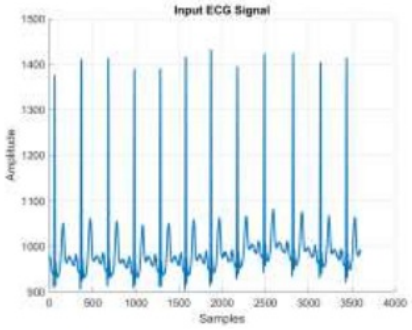
2	Extracted ECG Signal after filtering	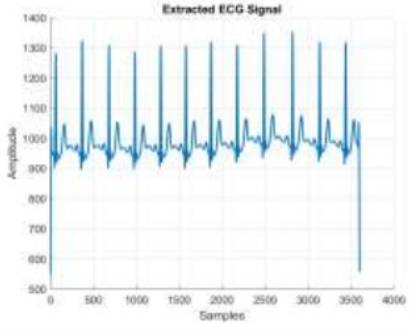

3	Extracting few peaks for better identification	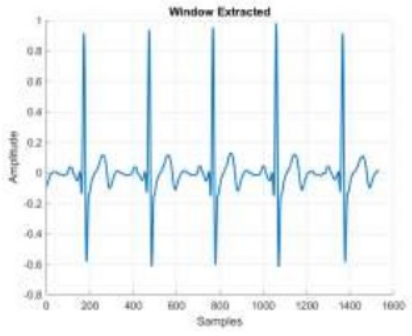
4	Inverting the signal for S peak extraction	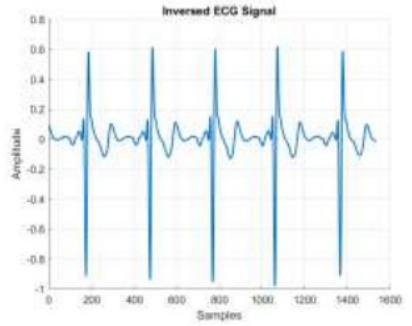
5	Detected P regions on the signal	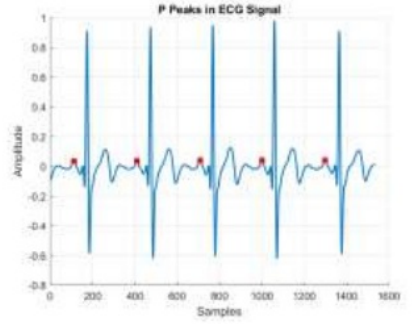
6	Detected R peaks in ECG	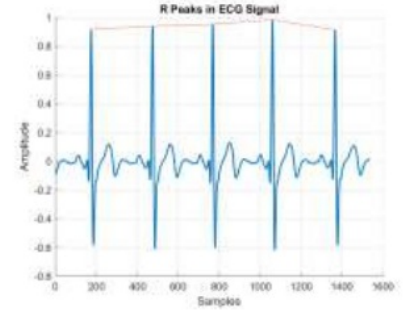

7	Detected S Peaks in ECG	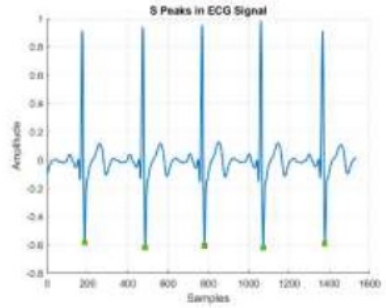
8	Detected T peaks in ECG	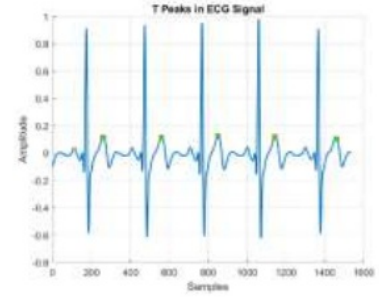
9	QRS Regions for generating BPM	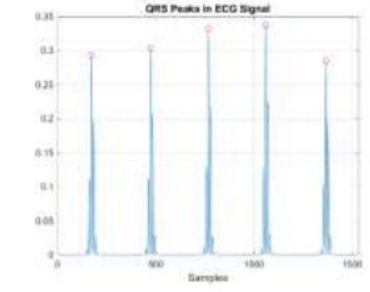

Table 5 ECG Analysis of Patient 5

No.	Figure Properties	Corresponding Figure
1	Input ECG File: 105m (0).mat Database: MIT Database Sampling Frequency: 360 Hz	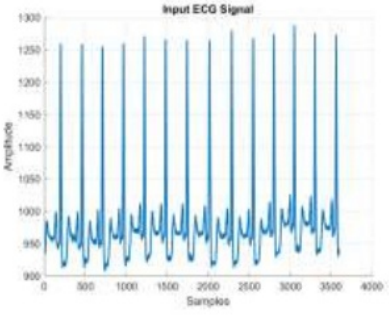

2	Extracted ECG Signal after filtering	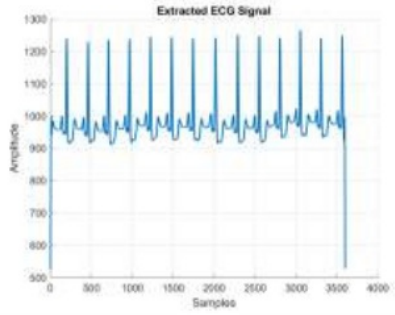
3	Extracting few peaks for better identification	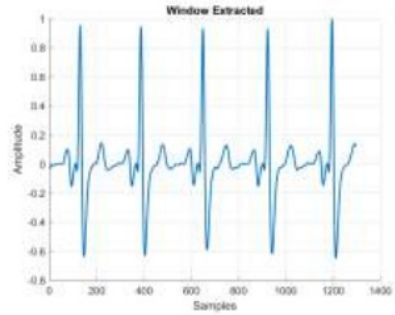
4	Inverting the signal for S peak extraction	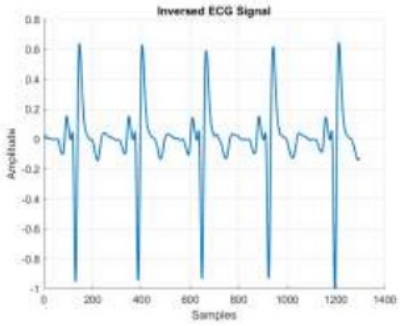
5	Detected P regions on the signal	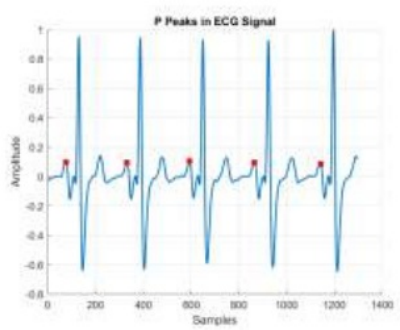

6	Detected R peaks in ECG	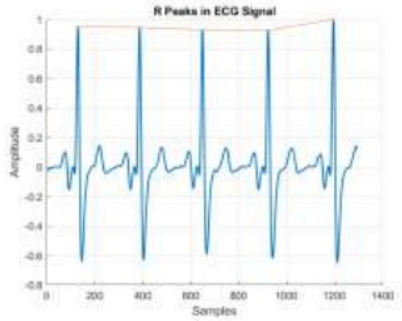
7	Detected S Peaks in ECG	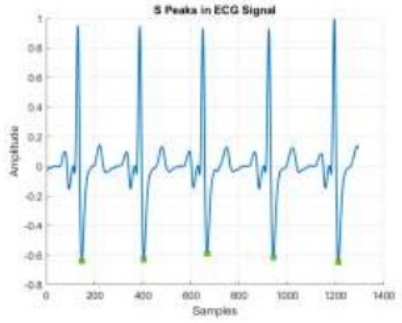
8	Detected T peaks in ECG	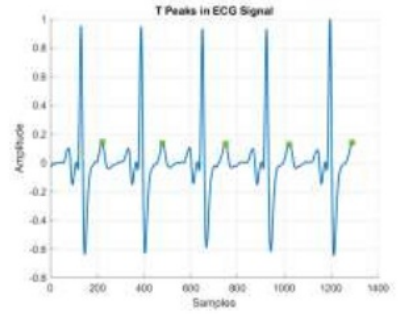
9	QRS Regions for generating BPM	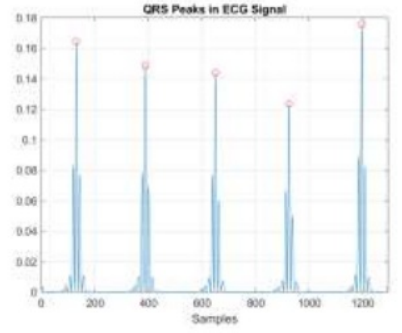

Table 6 ECG Analysis of Patient 6

No.	Figure Properties	Corresponding Figure
1	Input ECG File: 105m (1).mat Database: MIT Database Sampling Frequency: 360 Hz	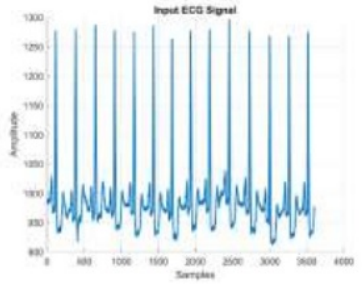
2	Extracted ECG Signal after filtering	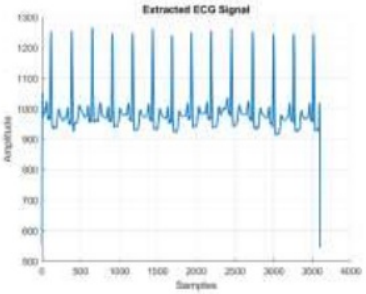
3	Extracting few peaks for better identification	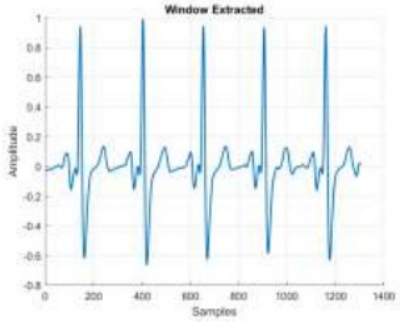
4	Inverting the signal for S peak extraction	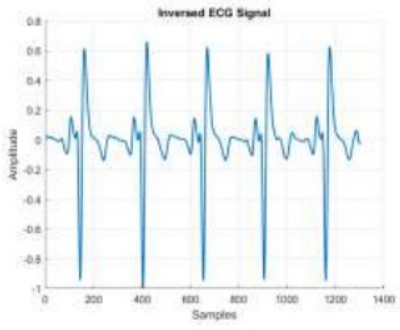

5	Detected P regions on the signal	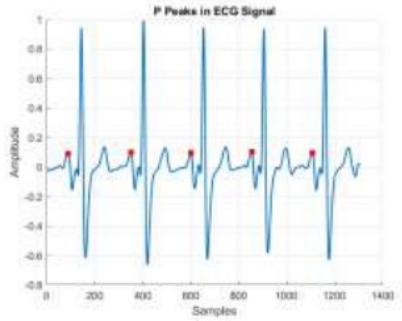
6	Detected R peaks in ECG	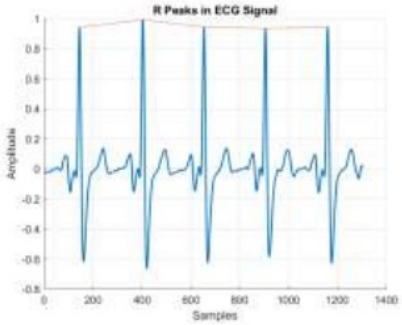
7	Detected S Peaks in ECG	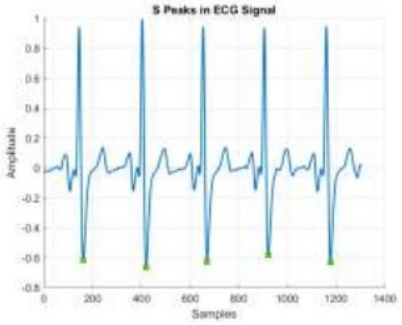
8	Detected T peaks in ECG	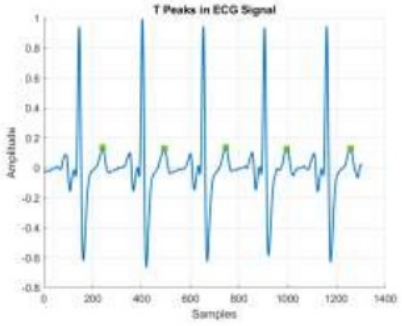

9	QRS Regions for generating BPM	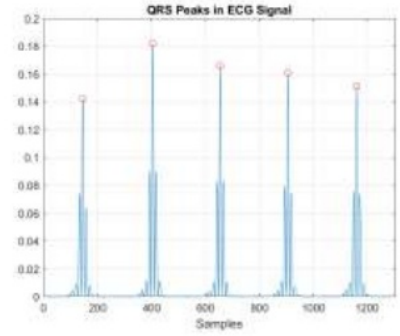

Table 7 ECG Analysis of Patient 7

No.	Figure Properties	Corresponding Figure
1	Input ECG File: 106m (1).mat Database: MIT Database Sampling Frequency: 360 Hz	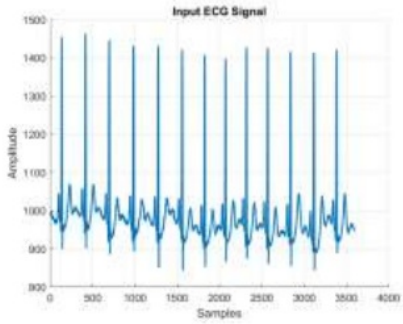
2	Extracted ECG Signal after filtering	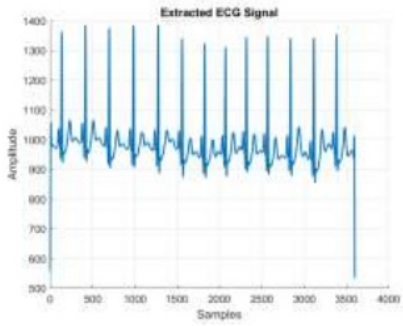

3	Extracting few peaks for better identification	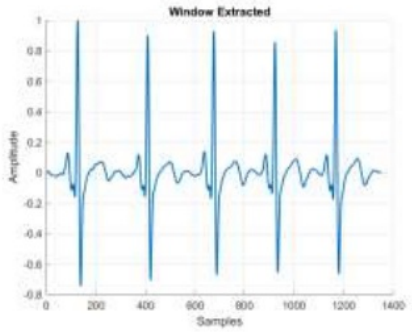
4	Inverting the signal for S peak extraction	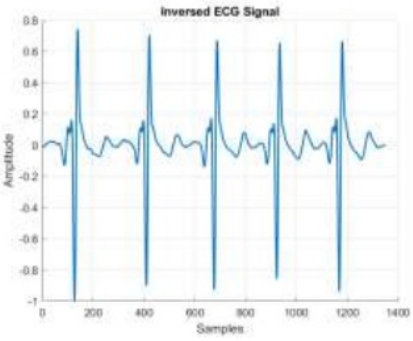
5	Detected P regions on the signal	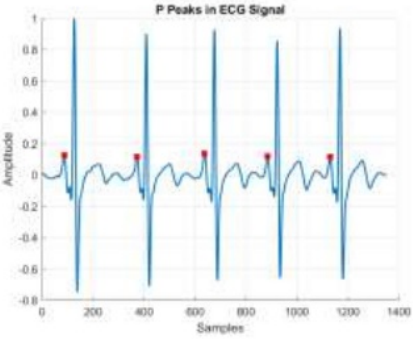
6	Detected R peaks in ECG	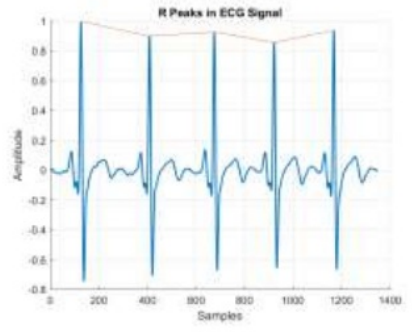

7	Detected S Peaks in ECG	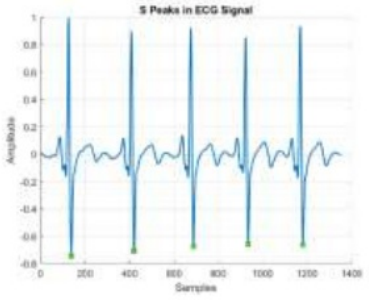
8	Detected T peaks in ECG	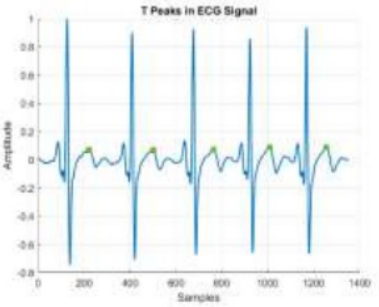
9	QRS Regions for generating BPM	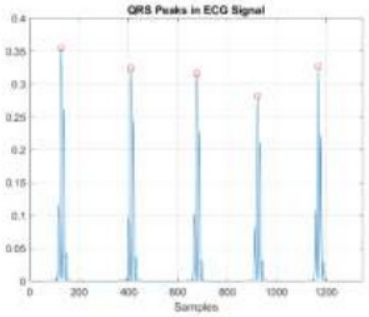

Table 8 ECG Analysis of Patient 8

No.	Figure Properties	Corresponding Figure
1	Input ECG File: 108m (0).mat Database: MIT Database Sampling Frequency: 360 Hz	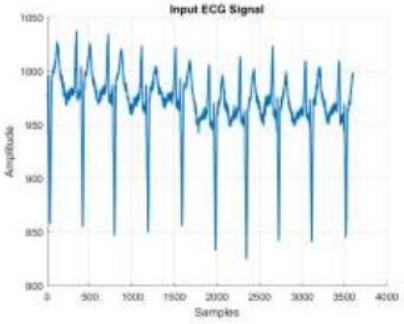

2	Extracted ECG Signal after filtering	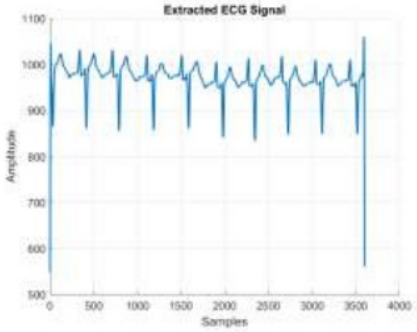
3	Extracting few peaks for better identification	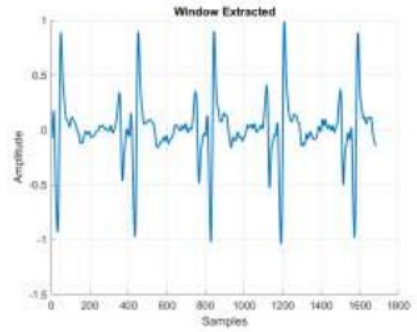
4	Inverting the signal for S peak extraction	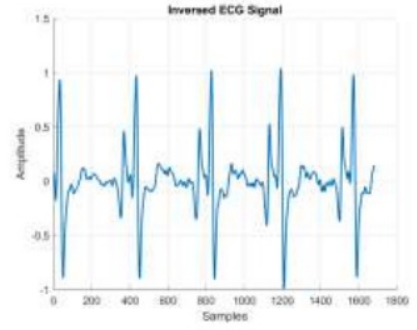
5	Detected P regions on the signal	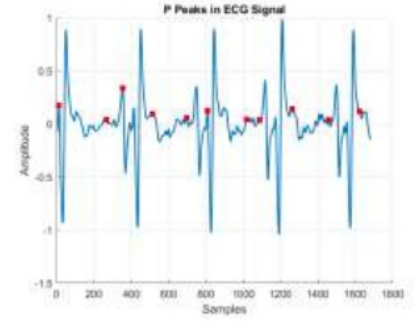

6	Detected R peaks in ECG	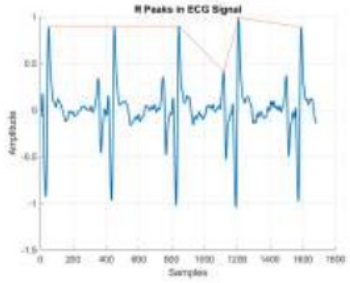
7	Detected S Peaks in ECG	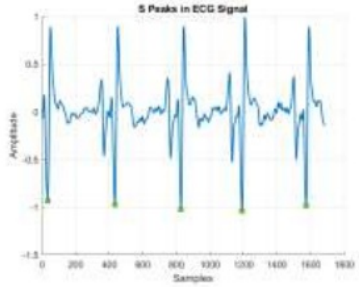
8	Detected T peaks in ECG	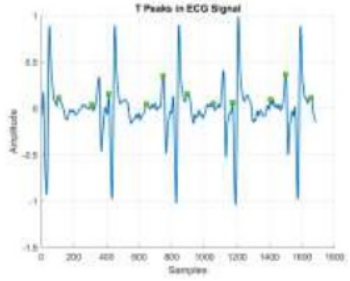
9	QRS Regions for generating BPM	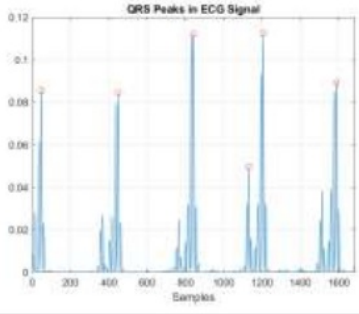

Table 9 ECG Analysis of Patient 9

No.	Figure Properties	Corresponding Figure
1	Input ECG File: 108m (4).mat Database: MIT Database Sampling Frequency: 360 Hz	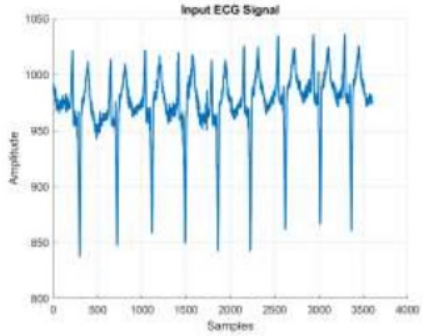
2	Extracted ECG Signal after filtering	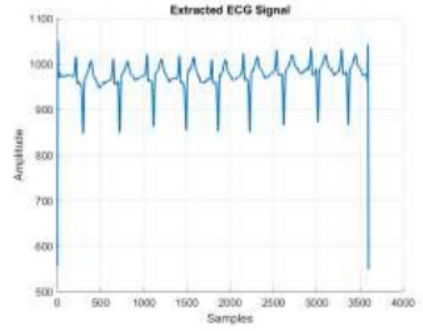
3	Extracting few peaks for better identification	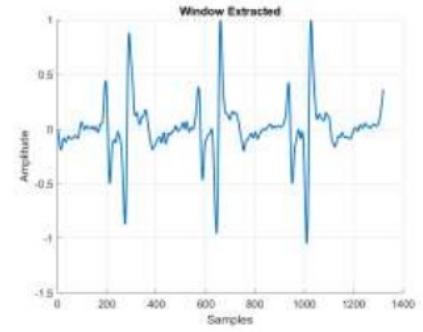
4	Inverting the signal for S peak extraction	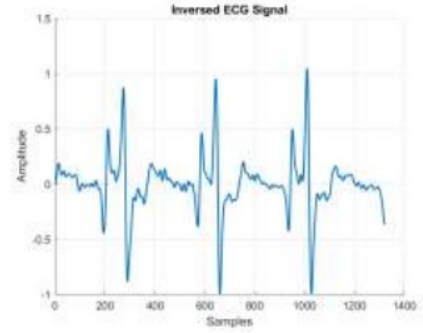

5	Detected P regions on the signal	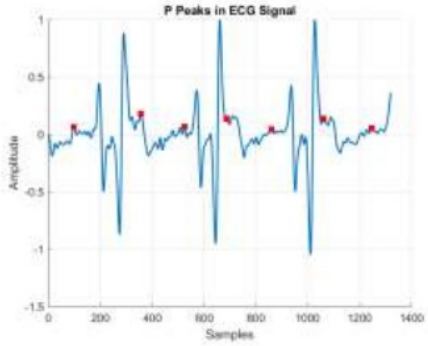
6	Detected R peaks in ECG	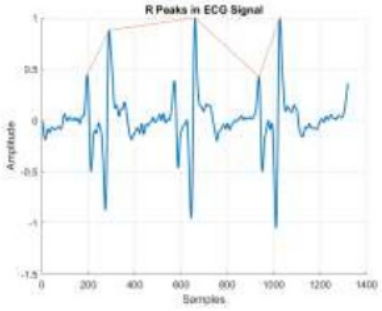
7	Detected S Peaks in ECG	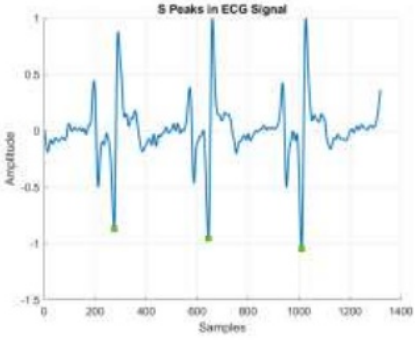
8	Detected T peaks in ECG	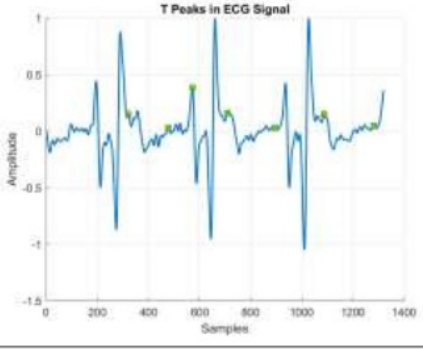

9	QRS Regions for generating BPM	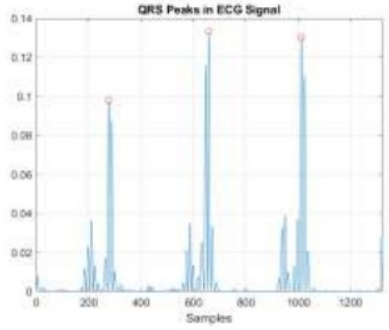

Table 10 ECG Analysis of Patient 1

No.	Figure Properties	Corresponding Figure
1	Input ECG File: 100m (2).mat Database: MIT Database Sampling Frequency: 360 Hz	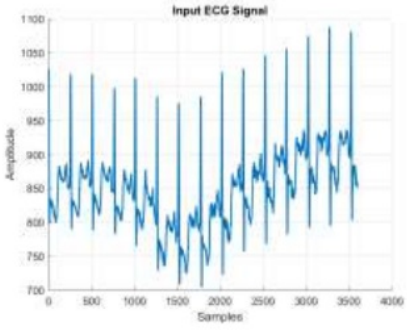
2	Extracted ECG Signal after filtering	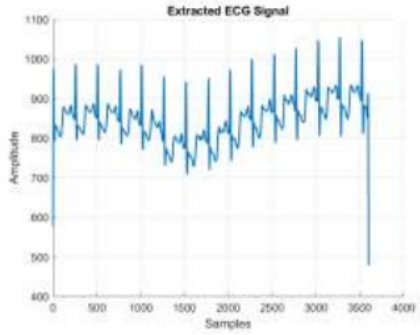

3	Extracting few peaks for better identification	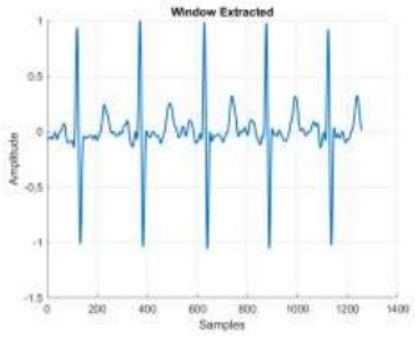
4	Inverting the signal for S peak extraction	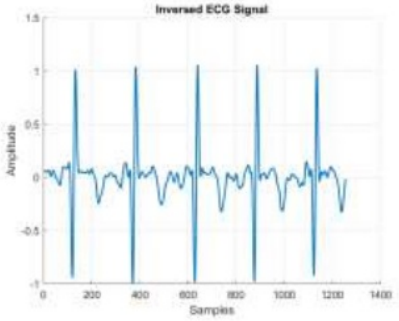
5	Detected P regions on the signal	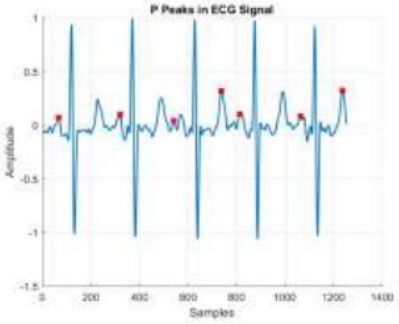
6	Detected R peaks in ECG	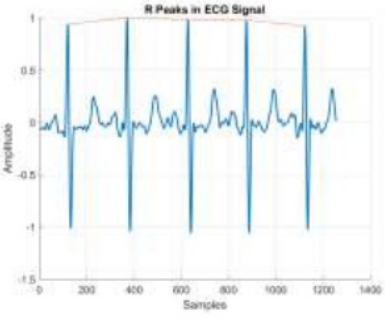

7	Detected S Peaks in ECG	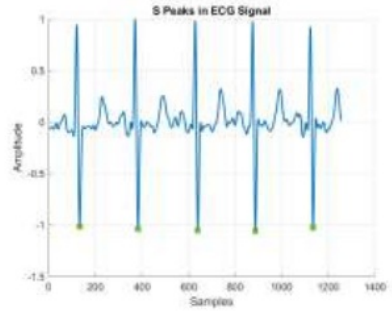
8	Detected T peaks in ECG	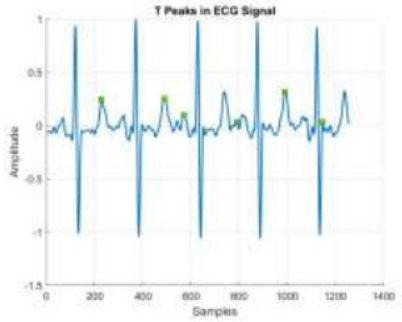
9	QRS Regions for generating BPM	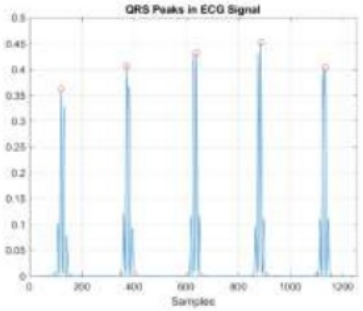

5.3 Accuracy and Precision of Our Proposed System

To compare our proposed method with previous works, we have measured the accuracy of our system first. Accuracy of a system can be measure by using following equations.

$$Accuracy = \frac{Number\ of\ correct\ predictions}{Total\ number\ of\ predictions}$$

As we are classifying information from an input ECG file, the accuracy equation can be written more sophisticatedly as,

$$Accuracy = \frac{TP + TN}{TP + TN + FP + FN}$$

Where,

TP stands for True Positive

TN stands for True Negative

FP stands for False Positive

FN stands for False Negative.

We have recorded all these parameters for 10 patients to verify our proposed system's performance.

Similarly, the Precision can be determined by using the following equation.

$$Precision = \frac{TP}{TP + FP}$$

Table 11 Recorded Data for P and T Peak Detection

No	File Name	TP	FN	TN	FP	Accuracy
1	100m (2).mat	5	0	5	0	1
2	101m (0).mat	5	0	5	0	1
3	103m (1).mat	5	0	5	0	1
4	103m (3).mat	5	0	5	0	1
5	105m (0).mat	5	0	5	0	1
6	105m (1).mat	5	0	5	0	1
7	106m (1).mat	5	0	5	0	1
8	108m (0).mat	2	9	3	8	0.2
9	108m (4).mat	0	7	2	5	0.1
10	112m (5).mat	4	3	3	3	0.5

Table 12 Recorded Data for QRS Detection

No	File Name	TP	FP	Precession
1	100m (2).mat	5	0	1
2	101m (0).mat	5	0	1
3	102m (1).mat	5	0	1
4	103m (3).mat	5	0	1
5	104m (0).mat	5	0	1
6	105m (1).mat	5	0	1
7	106m (1).mat	5	0	1
8	107m (0).mat	5	1	0.83
9	108m (4).mat	3	0	1
10	109m (5).mat	5	0	1

5.4 Comparison with Previous Work

The work proposed by Pratik D. Shertia ofr detecting R-peaks in ECG signal has an accuracy of 0.91 in QRS peak detection algorithm [30]. On another work proposed by Mounaim Aqil et. al. using wavelet analysis has achieved 0.99 detection accuracy for QRS peak [31]. The Neuro-fuzzy algorithm based on learning algorithm proposed by G. Rajender Naik et al., has achieved 0.88 accuracy which can be improve by adding more training data as this method proposed a learning based solution [12]. In biomedical area, a minor detection error can lead to a severe issue. In that case, our proposed technique has achieved overall 0.75 P and T wave detection accuracy but it has also achieved 0.983 precession accuracy for QRS peak detection which is a major standpoint.

Table 13 Comparison with Previous Works

Previous Methods	Technique	`Accuracy
Sensitivity and Positive Prediction Accuracy Analysis for R peak Detection in ECG Feature Extraction [30]	Part Average Testing (PAT) Algorithm	91.15%
Comparative Analysis of ECG Classification Using Neuro-Fuzzy Algorithm and Multimodal Decision Learning Algorithm [12]	Neuro-Fuzzy Algorithm and Multimodal Decision Learning Algorithm	81.25%
Our proposed method	Discrete Wavelet Transform (DWT)	98.30%

CHAPTER 6

CONCLUSIONS

6.1 Conclusions

This proposed work performs noise effects the performance of ECG peak detection algorithms. The performance of the algorithm has evaluated using the MIT-BIH Arrhythmia Database. This database has several examples of noisy ECGs and inaccurate annotations. These inaccurate annotations produced very low sensitivity results. A comparison of the performance has provided with the previous works. Evaluating the algorithms across the database shows the performance of various portion detections accuracy. The performance of the detectors drops and diverges when the ECG signal becomes utterly noisy. This highlights the significant opportunity for development and further research in this area.

6.2 Limitation of Our Thesis Work

The limitation of this work has discussed below.

- In certain condition when there is a very high noisy spike, the QRS detection algorithm fails to differentiate between noises and RR Peak.
- As P wave and T wave has similar properties, the algorithm in not always accurate specifically in these two areas.

6.3 Future Improvement

Some future work can be implemented later by further research has proposed below.

- Improving the performance of detecting P and T wave is still a very challenging task. There is a huge scope for improving these parts of the proposed algorithm.
- Adding machine learning algorithms like Deep Neural Network for analysis will improves the performance of the proposed system. Though there will be a necessity of huge dataset.

REFERENCES

[1] U. Satija, B. Ramkumar, and M. S. Manikandan, "Automated ECG noise detection and classification system for unsupervised healthcare monitoring," *IEEE J. Biomed. Heal. Informatics*, vol. 22, no. 3, pp. 722–732, May 2018, doi: 10.1109/JBHI.2017.2686436.

[2] R. Sharma, L. Vignolo, G. Schlotthauer, M. A. Colominas, H. L. Rufiner, and S. R. M. Prasanna, "Empirical Mode Decomposition for adaptive AM-FM analysis of Speech: A Review," *Speech Communication*, vol. 88. Elsevier B.V., pp. 39–64, Apr. 01, 2017, doi: 10.1016/j.specom.2016.12.004.

[3] M. Mneimneh and G. F. Corliss, "A cardiac electro-physiological model based approach for filtering high frequency ECG noise," in *Computers in Cardiology*, 2007, vol. 34, pp. 109–112, doi: 10.1109/CIC.2007.4745433.

[4] L. El Bouny, M. Khalil, and A. Adib, "ECG noise reduction based on stationary wavelet transform and zero-crossings interval thresholding," in *Proceedings of 2017 International Conference on Electrical and Information Technologies, ICEIT 2017*, Jan. 2018, vol. 2018-Janua, pp. 1–6, doi: 10.1109/EITech.2017.8255255.

[5] L. El Bouny, M. Khalil, and A. Adib, "ECG signal denoising based on ensemble emd thresholding and higher order statistics," Oct. 2017, doi: 10.1109/ATSIP.2017.8075546.

[6] M. S. Arulampalam, S. Maskell, N. Gordon, and T. Clapp, "A tutorial on particle filters for online nonlinear/non-Gaussian Bayesian tracking," *IEEE Trans. Signal Process.*, vol. 50, no. 2, pp. 174–188, Feb. 2002, doi: 10.1109/78.978374.

[7] H. D. Hesar and M. Mohebbi, "ECG Denoising Using Marginalized Particle Extended Kalman Filter with an Automatic Particle Weighting Strategy," *IEEE J. Biomed. Heal. Informatics*, vol. 21, no. 3, pp. 635–644, May 2017, doi: 10.1109/JBHI.2016.2582340.

[8] R. Sharma and S. R. Mahadeva Prasanna, "A better decomposition of speech obtained using modified Empirical Mode Decomposition," *Digit. Signal Process. A Rev. J.*, vol. 58, pp. 26–39, Nov. 2016, doi: 10.1016/j.dsp.2016.07.012.

[9] N. E. Huang *et al.*, "The empirical mode decomposition and the Hilbert spectrum for nonlinear and non-stationary time series analysis," *Proc. R. Soc. London. Ser. A Math. Phys. Eng. Sci.*, vol. 454, no. 1971, pp. 903–995, Mar. 1998, doi: 10.1098/rspa.1998.0193.

[10] A. Galli, G. Frigo, D. Chindamo, A. Depari, M. Gadola, and G. Giorgi, "Denoising ECG Signal by CSTFM Algorithm: Monitoring during Motorbike and Car Races," *IEEE Trans. Instrum. Meas.*, vol. 68, no. 7, pp. 2433–2441, Jul. 2019, doi: 10.1109/TIM.2019.2906989.

[11] P. Singh, S. Shahnawazuddin, and G. Pradhan, "Significance of modified empirical mode decomposition for ECG denoising," in *Proceedings of the Annual International Conference of the IEEE Engineering in*

Medicine and Biology Society, EMBS, Sep. 2017, pp. 2956–2959, doi: 10.1109/EMBC.2017.8037477.

[12] G. R. Naik and K. A. Reddy, "Comparative Analysis of ECG Classification Using Neuro-Fuzzy Algorithm and Multimodal Decision Learning Algorithm: ECG Classification Algorithm," in *Proceedings - 2016 3rd International Conference on Soft Computing and Machine Intelligence, ISCMI 2016*, Oct. 2017, pp. 138–142, doi: 10.1109/ISCMI.2016.35.

[13] R. Gutiérrez-Rivas, J. J. García, W. P. Marnane, and Á. Hernández, "Novel Real-Time Low-Complexity QRS Complex Detector Based on Adaptive Thresholding," *IEEE Sens. J.*, vol. 15, no. 10, pp. 6036–6043, Oct. 2015, doi: 10.1109/JSEN.2015.2450773.

[14] S. Mishra, D. Das, R. Kumar, and P. Sumathi, "A power-line interference canceler based on sliding DFT phase locking scheme for ECG signals," *IEEE Trans. Instrum. Meas.*, vol. 64, no. 1, pp. 132–142, Jan. 2015, doi: 10.1109/TIM.2014.2335920.

[15] D. G. Jang, S. H. Park, and M. Hahn, "A Gaussian model-based probabilistic approach for pulse transit time estimation," *IEEE J. Biomed. Heal. Informatics*, vol. 20, no. 1, pp. 128–134, Jan. 2016, doi: 10.1109/JBHI.2014.2372047.

[16] A. Sengur, "An expert system based on linear discriminant analysis and adaptive neuro-fuzzy inference system to diagnosis heart valve diseases," *Expert Syst. Appl.*, vol. 35, no. 1–2, pp. 214–222, Jul. 2008, doi: 10.1016/j.eswa.2007.06.012.

[17] A. Jovic and N. Bogunovic, "Analysis of ECG records using ECG chaos extractor platform and weka system," in *Proceedings of the International Conference on Information Technology Interfaces, ITI*, 2008, pp. 347–352, doi: 10.1109/ITI.2008.4588434.

[18] M. L. Smith, T. Kinugawa, and M. E. Dibner-Dunlap, "Reflex control of sympathetic activity during ventricular tachycardia in dogs: Primary role of arterial baroreflexes," *Circulation*, vol. 93, no. 5, pp. 1033–1042, Mar. 1996, doi: 10.1161/01.CIR.93.5.1033.

[19] J. J. Goldberger, "Sympathovagal balance: How should we measure it?," *Am. J. Physiol. - Hear. Circ. Physiol.*, vol. 276, no. 4 45-4, 1999, doi: 10.1152/ajpheart.1999.276.4.h1273.

[20] R. Mahajan and D. Bansal, "Identification of heart beat abnormality using heart rate and power spectral analysis of ECG," in *International Conference on Soft Computing Techniques and Implementations, ICSCTI 2015*, Jun. 2016, pp. 131–135, doi: 10.1109/ICSCTI.2015.7489555.

[21] A. Rabee and I. Barhumi, "ECG signal classification using support vector machine based on wavelet multiresolution analysis," in *2012 11th International Conference on Information Science, Signal Processing and their Applications, ISSPA 2012*, 2012, pp. 1319–1323, doi: 10.1109/ISSPA.2012.6310497.

[22] A. Ligtenberg and M. Kunt, "A robust-digital QRS-detection algorithm for arrhythmia monitoring," *Comput. Biomed. Res.*, vol. 16, no. 3, pp. 273–286, 1983, doi: 10.1016/0010-4809(83)90027-7.

[23] L. Biel, O. Pettersson, L. Philipson, and P. Wide, "ECG analysis: A new approach in human identification," *IEEE Trans. Instrum. Meas.*, vol. 50, no. 3, pp. 808–812, Jun. 2001, doi: 10.1109/19.930458.

[24] H. Baali, M. J. E. Salami, R. Akmeliawati, and A. M. Aibinu, "Analysis of the ECG signal using SVD-based parametric modelling technique," in *Proceedings - 2011 6th IEEE International Symposium on Electronic Design, Test and Application, DELTA 2011*, 2011, pp. 180–184, doi: 10.1109/DELTA.2011.60.

[25] A. A. S. Raj, N. Dheetsith, S. S. Nair, and D. Ghosh, "Auto analysis of ECG signals using artificial neural network," Feb. 2015, doi: 10.1109/ICSEMR.2014.7043597.

[26] R. V. Savitha, S. R. Breesha, and X. F. Joseph, "Pre processing the abdominal ECG signal using combination of FIR filter and principal component analysis," Jul. 2015, doi: 10.1109/ICCPCT.2015.7159460.

[27] "Counterstain - an overview | ScienceDirect Topics." https://www.sciencedirect.com/topics/biochemistry-genetics-and-molecular-biology/pq-interval (accessed Oct. 08, 2020).

[28] G. Coppola *et al.*, "ST segment elevations: Always a marker of acute myocardial infarction?," *Indian Heart Journal*, vol. 65, no. 4. Elsevier B.V., pp. 412–423, 2013, doi: 10.1016/j.ihj.2013.06.013.

[29] L. Cardone-Noott, A. Bueno-Orovio, A. Mincholé, N. Zemzemi, and B. Rodriguez, "Human ventricular activation sequence and the simulation of the electrocardiographic QRS complex and its variability in healthy and intraventricular block conditions," *Europace*, vol. 18, no. suppl_4, pp. iv4–iv15, Dec. 2016, doi: 10.1093/europace/euw346.

[30] P. D. Sherathia and V. P. Patel, "Sensitivity and positive prediction accuracy analysis for r peak detection in ECG feature extraction," in *2017 2nd International Conference for Convergence in Technology, I2CT 2017*, Dec. 2017, vol. 2017-Janua, pp. 680–685, doi: 10.1109/I2CT.2017.8226216.

[31] M. Aqil, A. Jbari, and A. Bourouhou, "Adaptive ECG Wavelet analysis for R-peaks detection," in *Proceedings of 2016 International Conference on Electrical and Information Technologies, ICEIT 2016*, Jul. 2016, pp. 164–167, doi: 10.1109/EITech.2016.7519582.

APPENDIX A

SOURCE CODE

```
clc

clear all

close all


sampling_freq   = 360; %as mentoined in database 100(m) are sampled at 360

ECG_file_value  = extractfield(ECG_file, 'val');

[ECG_file, d]   = lowpass(ECG_file_value,9/(sampling_freq/2)); %d=digital_filter; lowpass filter

%fvtool(d) %viewing the filter


%R peak extraction for windowing purpose

[peaks, locations_of_R] = findpeaks(ECG_filtered, 'MinPeakHeight', 0.4, 'MinPeakDistance', 90);

mean_RR_peak = mean(diff(locations_of_R)) / sampling_freq;

% fprintf('Mean RR peak: %f\n', mean_RR_peak);


%Window Extraction

if(length(locations_of_R) <= 6)

    ECG_filtered = ECG_filtered .* 1;

    ECG_inv      = -1 .* ECG_filtered;

else

    Number      = 5; %peaks to consider; standard; constant value

    window_1    = (round(mean_RR_peak * sampling_freq))* Number;

    idx         = locations_of_R(round(length(locations_of_R) / 2)) - round(window_1 / 2);

    ECG_filtered = ECG_filtered(bsxfun(@plus, idx, 0 : window_1 - 1));

    ECG_inv      = - ECG_filtered; %inversing the signal for opposite QRS Peak Detection

end
```

```
%Thresholding and peak finding
[peaks_3, locations_of_R_2] = findpeaks(ECG_filtered, 'MinPeakHeight', 0.4, 'MinPeakDistance', 90);
2, locations_of_S]   = findpeaks(ECG_inv, 'MinPeakHeight', 0.4, 'MinPeakDistance', 160); %Detecting S Peaks
[~, min_locations]        = findpeaks(ECG_inv, 'MinPeakHeight', 19); %Detecting Q Peaks
[locations_of_Q]          = min_locations(ECG_inv(min_locations)>0.12 & ECG_inv(min_locations)<0.3);
 %THresholding values



%P and T locations detemining
if(isempty(locations_of_PT) == 0)
    if(locations_of_PT(1) - locations_of_R_2(1) < 0 & locations_of_PT(2) - locations_of_R_2(1) > 0)

  elseif(locations_of_PT(1) - locations_of_R_2(1) < 0 & locations_of_PT(2) - locations_of_R_2(2) < 0)

  else
     locations_of_P = locations_of_PT(2:2:end);
     locations_of_T = locations_of_PT(1:2:end);
  end

else

end


%Eliminate noise and unwanted peak detection
if length(locations_of_S) >= length(locations_of_Q)
    locations_of_S_check = locations_of_S(1:length(locations_of_Q));
    check = any(locations_of_Q > locations_of_S_check);

```

```
    if(check == 1)
        locations_to_remove = find((locations_of_Q > locations_of_S_check) > 0 );
        locations_of_Q([locations_to_remove]) = [];
    end
end

%inherited from R-peak
no_of_samples_t = 1:length(ECG_filtered);
time_vector_tx = no_of_samples_t ./ sampling_freq;



ECG_signal_after_wavelet_y  = imodwt(ECG_wavelet_rec, 'sym4');

no_of_heart_beat = length(locations_of_R_from_wavelet);
time_limit = length(ECG_filtered) / sampling_freq;
heart_beat_per_minitue = (no_of_heart_beat * 60) / time_limit;

fprintf('Heart beat per minitue: %f\n', heart_beat_per_minitue);

%Ploting Data
fig_serial = 1;
figure(fig_serial); %original ECG signal
hold on
plot(ECG_file_value, 'linewidth', 1.5)
hold off
title('Input ECG Signal');
xlabel('Samples');
ylabel('Amplitude');
```

```
grid on
save_current_figure = figure(fig_serial);
saveas(fig_serial,sprintf('Figure_%d.png', fig_serial));
fig_serial = fig_serial+1;
grid on
save_current_figure = figure(fig_serial);
saveas(fig_serial,sprintf('Figure_%d.png', fig_serial));

fig_serial = fig_serial+1;
figure(fig_serial); %Filtered ECG signal
grid on
save_current_figure = figure(fig_serial);
saveas(fig_serial,sprintf('Figure_%d.png', fig_serial));

fig_serial = fig_serial+1;
figure(fig_serial); %Inversed ECG signal
hold on
plot(ECG_inv, 'linewidth', 1.5)
grid on
save_current_figure = figure(fig_serial);
saveas(fig_serial,sprintf('Figure_%d.png', fig_serial));

fig_serial = fig_serial+1;
figure(fig_serial); %P Peaks ECG signal
hold on
plot(ECG_filtered, 'linewidth', 1.5)
grid on
save_current_figure = figure(fig_serial);
```

```
saveas(fig_serial,sprintf('Figure_%d.png', fig_serial));


% fig_serial = fig_serial+1;
% figure(fig_serial); %Q Peaks ECG signal
% hold on
% plot(ECG_filtered, 'linewidth', 1.5)
% plot(locations_of_Q, ECG_filtered(locations_of_Q),'rs', 'MarkerFaceColor', 'g')
% hold off
% title('Q Peaks in ECG Signal');
% xlabel('Samples');
% ylabel('Amplitude');
% grid on
% save_current_figure = figure(fig_serial);
% saveas(fig_serial,sprintf('Figure_%d.png', fig_serial));
fig_serial = fig_serial+1;
figure(fig_serial); %R Peaks ECG signal
hold on
plot(ECG_filtered, 'linewidth', 1.5)
plot(locations_of_R_2, ECG_filtered(locations_of_R_2))
hold off
title('R Peaks in ECG Signal');
xlabel('Samples');
ylabel('Amplitude');
grid on
save_current_figure = figure(fig_serial);
saveas(fig_serial,sprintf('Figure_%d.png', fig_serial));
fig_serial = fig_serial+1;
figure(fig_serial); %S Peaks ECG signal
```

```
hold on
plot(ECG_filtered, 'linewidth', 1.5)
plot(locations_of_S, ECG_filtered(locations_of_S),'rs', 'MarkerFaceColor', 'g')
hold off
title('S Peaks in ECG Signal');
xlabel('Samples');
ylabel('Amplitude');
grid on
save_current_figure = figure(fig_serial);
saveas(fig_serial,sprintf('Figure_%d.png', fig_serial));
fig_serial = fig_serial+1;
figure(fig_serial); %S Peaks ECG signal
hold on
plot(ECG_filtered, 'linewidth', 1.5)
plot(locations_of_T, ECG_filtered(locations_of_T),'rs', 'MarkerFaceColor', 'g')
hold off
title('T Peaks in ECG Signal');
xlabel('Samples');
ylabel('Amplitude');
grid on
save_current_figure = figure(fig_serial);
grid on
xlim([0, length(ECG_filtered)])
hold on
plot(locations_of_R_from_wavelet, R_peak_from_wavelet, 'ro')
xlabel('Samples')
save_current_figure = figure(fig_serial);
title('QRS Peaks in ECG Signal');
```

```
saveas(fig_serial,sprintf('Figure_%d.png', fig_serial));


% bpm = round(60/RR_mean);


%QRS Period
QRS_period =[];


if length(locations_of_Q) > length(locations_of_S)
    locations_of_Q_1 = locations_of_Q(1:length(locations_of_S));
    locations_of_S_1 = locations_of_S;

else
    locations_of_S_1 = locations_of_S(1:length(locations_of_Q));
    locations_of_Q_1 = locations_of_Q;

end


for j = 1:max(length(locations_of_Q_1),length(locations_of_S_1))
    QRS_period(j) = (locations_of_S_1(j) - locations_of_Q_1(j));
end


QRS_mean = mean(QRS_period)/sampling_freq;


if isnan(QRS_mean) == 1
    QRS_mean = 0;
end


% fprintf('Mean QRS peak: %f\n', QRS_mean);
```

```
%PR interval-----------------------------------------------------------------

PR_interval = [];

temp = 0;


if length(locations_of_R_2) > length(locations_of_P)

    locations_of_R_3 = locations_of_R_2(1:length(locations_of_P));

    locations_of_R_2 = locations_of_P;

    temp =1;

else

    locations_of_P_2 = locations_of_P(1:length(locations_of_R_2));

    locations_of_R_3 = locations_of_R_2;

    temp =1;

end




for k = 1 :max(length(locations_of_R_3),length(locations_of_P_2))

    PR_interval(k) = locations_of_R_3(k) - locations_of_P(k);


end

if temp ==0

    mean_PR = mean(PR_interval)/sampling_freq;

elseif temp ==1

    mean_PR = abs(mean(PR_interval))/sampling_freq;

end


if isnan(mean_PR) == 1

    mean_PR = 0;
```

```
end


fprintf('Mean PR peak: %f\n', mean_PR);



%QT interval-----------------------------------------------------------------
QT_interval = [];
if length(locations_of_Q) > length(locations_of_T)
    locations_of_Q_2 = locations_of_Q(1:length(locations_of_T));
    locations_of_T_2 = locations_of_T;
    flag =1;

else
    locations_of_T_2 = locations_of_T(1:length(locations_of_Q));
    locations_of_Q_2 = locations_of_Q;
    flag =1;
end



for k = 1 :max(length(locations_of_Q_2),length(locations_of_T_2))
    QT_interval(k) = locations_of_T_2(k) - locations_of_Q_2(k);

end
if flag ==0
    mean_QT = mean(QT_interval)/sampling_freq;
elseif flag == 1
    mean_QT = abs(mean(QT_interval))/sampling_freq;
end
```

```
if isnan(mean_QT) ==1
    mean_QT = 0;
end
% fprintf('Mean QT peak: %f\n', mean_QT);
```

2020_12_04_ECG_ANALYSIS_REPORT_U

ORIGINALITY REPORT

5%	4%	3%	2%
SIMILARITY INDEX	INTERNET SOURCES	PUBLICATIONS	STUDENT PAPERS

PRIMARY SOURCES

1	www.archive.org Internet Source	1%
2	T.P. Pander. "A suppression of an impulsive noise in ECG signal processing", The 26th Annual International Conference of the IEEE Engineering in Medicine and Biology Society, 2004 Publication	1%
3	www.heart.org Internet Source	1%
4	dspace.mit.edu Internet Source	<1%
5	bitsavers.trailing-edge.com Internet Source	<1%
6	Submitted to Asia Pacific University College of Technology and Innovation (UCTI) Student Paper	<1%
7	hdl.handle.net Internet Source	<1%

8	www.olympedegouges.eu Internet Source	<1%
9	Submitted to Endeavour College of Natural Health Student Paper	<1%
10	www.lm.doe.gov Internet Source	<1%
11	aquaticcommons.org Internet Source	<1%
12	publications.iowa.gov Internet Source	<1%
13	cmgds.marine.usgs.gov Internet Source	<1%
14	Friedrich Münzinger. "Ingenieure Baumeister Einer Besseren Welt", Springer Science and Business Media LLC, 1947 Publication	<1%

Exclude quotes	On	Exclude matches	Off
Exclude bibliography	On		